

#036

SOURCE TARGET & LIST, TIME & RA ORDER

77-075A-02C

EXTRAGALACTIC X-RAY SOURCE CATALOG

77-075A-02E

77-075A-02D

HEAO 1

HEAD 1

NEW HARD X-RAY SOURCES

77-075A-02D

THIS DATA SET HAS BEEN RESTORED. ORIGINALLY THERE WAS ONE 9-TRACK, 1600 BPI TAPE. THERE IS ONE RESTORED TAPE. THE TAPE CONTAINS TWO FILES OF DATA, THE FIRST FILE IS ASCII AND THE SECOND FILE IS EBCDIC. THE TAPE WAS CREATED ON AN IBM 360 COMPUTER. THE DR TAPE IS A 3480 CARTRIDGE AND THE DS TAPE IS 9-TRACK, 6250 BPI. THE DR AND DS NUMBERS ALONG WITH THE CORRESPONDING D NUMBERS ARE AS FOLLOWS:

DR#	DS#	D#	FILES	TIME SPAN
DR03716	DS03716	D45319	2	09/01/77 - 03/09/78

REQ. AGENT

LSM

RD #

V0088

ACQ. AGENT

MCL

HEAO 1

NEW HARD X RAY SOURCES

77-075A-02D

This data set consists of one data tape. It is 1600 bpi, 9 track with two files. The files are identical but the first file is in ASCII and the second file is in EBCDIC. This tape contains a listing of TABLE 2 of the paper " New Hard X-Ray Soures Observed with HEAO A2 ". The table contains the positions and intensities of these sources. The 'D' and 'C' numbers and time span follow:

<u>D#</u>	<u>C#</u>	<u>TIME SPAN</u>
D-4519	C-21559	9/1/77 - 3/9/78

Enclosure 1

The tape is 9 track, 1600 bpi. It contains two files which are identical except that the first is in ASCII and the second is in EBCDIC. The logical record size is 124 bytes. Each logical record is an image of a line normally printed on a line printer. The physical blocksize is 2480 bytes. The blocking format is FB.

Two lines of data are given for each source. The data are formatted as follows:

Line 1:

<u>Columns</u>	<u>Format</u>	<u>Content</u>
3	A1	'H'
4-7	I4	Right Ascension
8-11	I4	Declination
14-20	F7.2	Right Ascension
21-27	F7.2	Galactic Longitude
29-56	4F7.2	Right Ascension of Box 1
58-85	4F7.2	Right Ascension of Box 2
86-91	F6.2	Size of Error Box 1
92-98	F7.2	Intensity
99-104	F6.0	Day of Observation
109-124	16A1	Comments

Line 2:

14-20	F7.2	Declination
21-27	F7.2	Galactic Latitude
29-56	4F7.2	Declination of Box 1
58-85	4F7.2	Declination of Box 2
86-91	F6.2	Size of Error Box 2
109-124	16A1	Comments

X-1906

D-45319

SEXE TPLIST BS

INPUT PARAMETERS ARE: AS FL=1=1

TAPE NO. 1 FILE NO. 1  
RECORD 1 LENGTH 2480

TABLE 2.

LIST OF SOURCES.

L	BOX1	BOX2	SIZE 1	INT.	DAY	NAME	RA
(10)	(11)	(12)	(13)	(14)	(15)	(2)	(9)
1977	DEC	B	1950	RA/DEC	(3)		
			1950	RA/DEC	(6)	SIZE 2	

H0008+105	2.12	107.12	4.97	359.39	359.16	4.75	1.67	1.44	2.57	2.79	3.30	1.6
4 362.	1117W2**				10.54	-50.81	11.45	9.04	9.54	11.95	10.05	10.55
11.04	10.53	0.64										

03.06	16.68	7.75	5.64	15.02	12.39	10.48	11.88	13.70	3.60	4.40	302.54	18.96	10.71	7

75	16.68	14.48	11.76	12.52	15.15	4.80	4.70	307.	SMCX-2**					

4	18.65	18.90	3.60	1.49	367.	AB151*	17.87	146.87	15.35	21.03	20.77	15.11	17.10	16.8

TAPE NO. 1 FILE NO. 1  
RECORD 12 LENGTH 620

UNFIRMED USING 3 DEGREE FOV.  
NOTE 2: SOURCE NEAR NORTHERN ECLIPTIC POLE--NO BOX 2 DETERMINED.

\*\*\*\*\* JOB DONE.  
\$WEO LPS

NOTE 1: THIS SOURCE CO





HEAD 1

SOURCE TARGET LIST, TIME & RA ORDERED

77-075A-026

THIS DATA SET HAS BEEN RESTORED. ORIGINALLY THERE WAS ONE 9-TRACK, 6250 BPI TAPE WRITTEN IN EBCDIC WITH 3 BINARY HEADER RECORDS. THERE IS ONE RESTORED TAPE. THE DR TAPE IS A 3480 CARTRIDGE AND THE DS TAPE IS 9-TRACK, 6250 BPI. THE TAPE WAS CREATED ON AN IBM 3081 COMPUTER. THE DR AND DS NUMBERS ALONG WITH THE CORRESPONDING D NUMBER AND THE TIME SPAN IS AS FOLLOWS:

DR#	DS#	D#	FILES	TIME SPAN
DR03674	DS03674	D59881	1	11/15/77 - 12/29/78



REQ. AGENT  
DAD

RAND #  
V0215

ACQ. AGENT  
HKH

HEAO-1

SOURCE TARGET LIST, TIME & RA ORDERED

77-075A-02G

This data set contains one magnetic tape. It is 6250 BPI, 9 track, has 1 file and is written in EBCDIC with 3 binary header records, it was created on the 3081. The C tape is 1600 BPI.

<u>D#</u>	<u>C#</u>	<u>TIME SPAN</u>
D-59881	C-23463	11/15/77 - 12/29/78

July 20, 1983

TO: 601/Director (J. Vette)  
National Space Science Data Center (NSSDC)

FROM: 660/HEAO-1 A2 Experiment  
F. Marshall

SUBJECT: HEAO-1 A2 Data Submission

Enclosed are two lists of the targets that the HEAO A2 experiment pointed at during its mission. The lists are identical except that one is ordered by time and the other is ordered by right ascension of the y-axis. Each list has ten columns of information:

- 1) target name
- 2) whether the target was on the +y or -y side of the spacecraft  
(note that the A2 experiment only viewed the +y targets)
- 3) R.A. of y-axis (1950 epoch)
- 4) Dec. " "
- 5) Day of 1977 of start of point
- 6) Second " " " "
- 7) Day of 1977 of end of "
- 8) Second " " " "
- 9) 'PP' indicates spacecraft alternated between two positions during point.
- 10) point number

Also enclosed is a magnetic tape containing these lists and documentation on how to read the tape.

*F. E. Marshall*

Francis E. Marshall  
Laboratory for High Energy Astrophysics

Enclosures

cc: E. Boldt/661  
S. Holt/660

*TWO PRINTED LISTS  $\equiv$  data  
on magnetic tape  
 $\Rightarrow$  only the 1st page of each  
list was preserved in this  
package. (CYN, 9/96)*

MM-075A-026

Enclosure 1

The tape is 9 track, 6250 bpi and was written with the SACC IBM 3081.

It contains one file which is copy of a partitioned data set containing two members. It can be read using the following JCLs:

```
// EXEC IEBCOPY
//SYSUT1 DD DSN=POINT.LIST,DISP=OLD,
// LABEL=(1,NL,,IN),VOL=SER=XXXXX,
// DCB=(DEN=4),UNIT=6250
//SYSUT2 DD DSN=ZBMEN.POINT.LIST,
// DISP=SHR
//SYSUT3 DD SPACE=(1,10),UNIT=SYSDA
//SYSUT4 DD SPACE=(1,10),UNIT=SYSDA
//SYSPRINT DD SYSOUT=A
//SYSIN DD DUMMY
```

INPUT TAPF DOUT2 ON TUE  
DATA INPUT P9 FL 1 3 3

3 Reads  
as follows

FILE	RECORD	LENGTH	BYTES
FILE 01	RECORD 1	LENGTH 284	BYTES 284
( 0 )	01C00000	01180000	FF000000
( 40 )	00000000	00000000	00000000
( 80 )	00000000	00000000	00000000
( 120 )	00000000	00000000	00000000
( 160 )	00000000	00000000	00000000
( 200 )	00000000	00000000	00000000
( 240 )	00000000	00000000	00000000
( 280 )	00000000	00000000	00000000

FILE	RECORD	LENGTH	BYTES
FILE 01	RECORD 2	LENGTH 296	BYTES 296
( 0 )	01240000	00000000	00000000
( 40 )	05C0E0C1	00000000	0400FFFF
( 80 )	00000000	00000000	00000000
( 120 )	00000000	00000000	00000000
( 160 )	00000000	00000000	00000000
( 200 )	00000000	00000000	00000000
( 240 )	00000000	00000000	00000000
( 280 )	00000000	00000000	00000000

FILE	RECORD	LENGTH	BYTES
FILE 01	RECORD 3	LENGTH 730	BYTES 730
( 0 )	1C840000	1C800000	00180006
( 40 )	4E324CF1	F9F449F8	F14BF3F3
( 80 )	4C404040	40404040	F0F2E4F4
( 120 )	4E3E40F1	F9F449F8	F14BF3F7
( 160 )	4C404040	40404040	F0F0F0F0
( 200 )	60E940F1	F9F540F2	F140F1F0
( 240 )	40404040	40404040	F0F2F7F4
( 280 )	4E3E40F1	F9F640F5	F0F5F3F6

FILE	RECORD	LENGTH	BYTES
( 0 )	1C840000	1C800000	00180006
( 40 )	4E324CF1	F9F449F8	F14BF3F3
( 80 )	4C404040	40404040	F0F2E4F4
( 120 )	4E3E40F1	F9F449F8	F14BF3F7
( 160 )	4C404040	40404040	F0F0F0F0
( 200 )	60E940F1	F9F540F2	F140F1F0
( 240 )	40404040	40404040	F0F2F7F4
( 280 )	4E3E40F1	F9F640F5	F0F5F3F6
( 320 )	40404040	40404040	F0F1F6F8
( 360 )	4E3E40F1	F9F640F5	F0F7E2F7
( 400 )	40404040	40404040	F0F4F5F5
( 440 )	4E3E40F1	F9F740F5	F0F7E2F7
( 480 )	40404040	40404040	F0F4F5F5
( 520 )	4E3E40F1	F9F840F5	F0F7E2F7
( 560 )	40404040	40404040	F0F4F5F5
( 600 )	60E840F1	40404040	F34BF7F8
( 640 )	4C404040	40404040	F0F0F0F0
( 680 )	60E840F1	F9F840F5	F440F0F7
( 720 )	40404040	40404040	F0F0F0F0
( 760 )	4E3E40F2	F0F040F5	F24BF7F8
( 800 )	40404040	40404040	F0F0F0F0
( 840 )	4E3E40F2	F0F040F5	F24BF7F8
( 880 )	40404040	40404040	F0F0F0F0
( 920 )	60E840F2	F0F040F5	F24BF7F8
( 960 )	40404040	40404040	F0F0F0F0
( 1000 )	4E3E40F2	F0F040F5	F24BF7F8
( 1040 )	40404040	40404040	F0F0F0F0
( 1080 )	4E3E40F2	F0F040F5	F24BF7F8
( 1120 )	40404040	40404040	F0F0F0F0
( 1160 )	4E3E40F2	F0F040F5	F24BF7F8
( 1200 )	40404040	40404040	F0F0F0F0
( 1240 )	4E3E40F2	F0F040F5	F24BF7F8
( 1280 )	40404040	40404040	F0F0F0F0
( 1320 )	4E3E40F2	F0F040F5	F24BF7F8

4-10

D-59281



\*\*\*\* TSD FOREGROUND HARD COPY \*\*\*\*  
 DSNNAME=ZBMEN.POINT.LIST

(TIME )

TEST POINT	167.25	58.00	31.9	16933	31.9	28764	04000001
SMCX-1	19.20	73.60	320	64338	320	76360	00000002
CVG X-1	299.12	35.06	321	67621	321	79677	00000003
AT54	135.70	49.50	322	76943	322	2302	00000004
VELA P	308.70	45.10	327	69084	327	80084	00000005
MK421	345.88	38.27	333	59273	333	69936	00000006
VELA PULSAR	128.70	45.10	335	54041	335	64606	00000007
NGC4151	182.00	39.80	340	46229	340	57016	00000008
2A0922	140.50	31.70	341	43749	341	54326	00000009
SS CYGNI	325.18	43.36	350	7446	350	19480	00000010
BLLAC	149.11	42.13	355	63198	355	77620	00000011
3C273	7.16	12.08	357	60538	357	74972	00000012
M87	187.01	13.66	362	57858	362	72146	00000013
H7A3	278.30	23.22	369	70454	369	82407	00000014
AU0050-01	12.03	1.99	369	57780	369	79267	00000015
NGC278	14.28	3.81	374	57443	374	69262	00000016
3C279	13.40	5.52	374	64601	374	66857	00000017
UVCEI 1	24.00	18.22	375	51586	375	72268	00000018
CEN X-3	169.76	60.35	378	58794	378	69562	00000019
NDVA(3U015+63)	18.80	63.47	381	50755	381	62465	00000020
CAS A	350.30	58.55	382	48368	381	59013	00000021
CEN A	200.63	42.78	390	51551	382	62161	00000022
GX301-2	185.92	62.49	390	46027	384	57959	00000023
M-31	190.01	41.00	396	46198	390	58050	00000024
GX301-2	185.95	62.49	398	64501	396	76447	00000025
CEN A	5.95	62.49	398	67661	397	83043	00000026
AU0336+01	21.48	43.08	399	70967	398	85217	00000027
TYCHO	054.50	00.53	402	62323	399	78567	00000028
A 401 1275	185.60	63.88	405	59915	402	74126	00000029
NGC 401	43.65	13.25	404	57030	403	74372	00000030
GX304-1	49.15	41.35	405	54247	404	68660	00000031
TYCHO	22.96	13.31	410	51493	405	65779	00000032
CTR X-1	194.57	61.37	411	3236	410	14582	00000033
A1540-53	5.60	63.88	412	64480	411	72960	00000034
NGC 1275	229.20	56.99	413	64440	412	76074	00000035
UX ARI	235.30	53.40	416	59053	413	79320	00000036
HER X-1	228.72	41.25	417	70814	416	70814	00000037
HER X-1	219.80	61.45	418	65294	417	67944	00000038
HER X-1	50.88	28.54	419	55262	418	75854	00000039
HER X-1	254.01	36.42	420	66490	419	73025	00000040
HER X-1	254.01	35.42	424	53863	420	66542	00000041
MSH14-63	247.94	37.31	425	59237	423	67806	00000042
MK 501	219.05	61.21	429	58561	425	70893	00000043
HER X-1	72.63	41.82	427	53460	429	68930	00000044
HER X-1	254.01	35.42	430	52810	427	65337	00000045
MXB 1728-34	262.20	33.80	432	48011	427	64774	00000046
MXB 1728-34	82.20	33.80	433	2707	431	59819	00000047
MXB 1659-29	75.75	29.90	438	66058	432	16650	00000048
MXB 1728-34	82.20	33.80	439	66299	434	59819	00000049
4U1626-67	82.20	33.80	439	68340	433	77199	00000050
4U0517+17	67.11	67.63	440	66299	434	80176	00000051
3C129	254.14	38.34	445	65986	438	77338	00000052
BACKGROUND	250.95	46.94	446	65071	439	77849	00000053
CRAB(4U0531+21)	23.84	38.34	447	63071	439	83320	00000054
GA14	84.46	21.98	448	66627	440	80461	00000055
BACKGROUND	262.20	24.70	452	66627	445	6348	00000056
AMHER	273.74	49.85	452	57806	445	84606	00000057
4U1626-67	274.49	43.87	452	72185	446	74109	00000058
H1743-32	246.60	67.38	453	72185	447	84132	00000059
MXB 1730-32(BURSTER)	262.53	32.65	455	50402	452	18307	00000060
JUPITER	268.47	23.36	457	50402	452	18307	00000061
3C390.3	101.55	80.00	458	50402	452	18307	00000062
4U1847+78	107.31	80.00	458	50402	452	18307	00000063
CG195+4	99.00	17.50	459	50402	452	18307	00000064
LMCX-1	085.10	59.8	461	50402	452	18307	00000065
3C390.3	101.35	80.00	465	50402	452	18307	00000066
4U1847+78	98.31	78.09	465	50402	452	18307	00000067
2A1914-589	289.20	58.82	466	50402	452	18307	00000068
2A1914-589	291.20	65.10	466	50402	452	18307	00000069

77-075A-029  
 Provided by P.I.



HEAO 1

Extragalactic X-Ray Source Catalog

77-075A-02E

This data set has been restored. Originally there was one 9-track, 1600 BPI tape written in ASCII. There is one restored tape. The DR tape is a 3480 cartridge and the DS tape is a 9-track, 6250 BPI tape. The tape was created on a 3081 computer. The DR and DS numbers, along with the corresponding D number and the time span follow.

DR#	DS#	DD#	Files	Time Span
DR03672	DS03672	D48693	1	09/05/77 - 09/11/78



REQ. AGENT  
DAD

RAND #  
V0215

ACQ. AGENT  
HKH

HEAO-1

EXTRAGALACTIC X-RAY SOURCE CATALOG

77-075A-02E

This data set contains one magnetic tape. It is 1600 BPI, 9 track, written in ASCII, has 1 file and was created on the 3081. The time span is not found on the tape but, is contained in the documentation.

D#

C#

TIME SPAN

D-46893

C-23462

9/05/77 - 9/11/78

ENCLOSURE 1

The tape is 9 track, 1600 bpi. It contains one file which is in ASCII. The logical record size is 120 bytes. Each logical record is an image of a line normally printed on a line printer. The physical blocksize is 2400 bytes. The blocking format is FB.

B33286-000H

DLO=X

HCK=D

77-01571-020



Technical Memorandum 82168

**A Complete X-Ray Sample of the  
High Latitude ( $|b| > 20^\circ$ ) Sky from  
HEAO -1 A-2: Log N - Log S  
and Luminosity Functions**

**G. Piccinotti, R. F. Mushotzky, E.A. Boldt,  
S. S. Holt F. E. Marshall, P. J. Serlemitsos  
and R. A. Shafer**

**AUGUST 1981**

National Aeronautics and  
Space Administration

**Goddard Space Flight Center**  
Greenbelt, Maryland 20771

A COMPLETE X-RAY SAMPLE OF THE HIGH LATITUDE ( $|b| > 20^\circ$ )  
SKY FROM HEAO-1 A-2: LOG N - LOG S AND LUMINOSITY FUNCTIONS

G. Piccinotti<sup>1</sup>, R.F. Mushotzky, E.A. Boldt, S.S. Holt,  
F.E. Marshall, P.J. Serlemitsos and R.A. Shafer<sup>2</sup>

Laboratory for High Energy Astrophysics  
NASA/Goddard Space Flight Center  
Greenbelt, Maryland 20771

ABSTRACT

The HEAO-1 experiment A-2 has performed a complete X-ray survey of the 8.2 steradians of the sky at  $|b| > 20^\circ$  down to a limiting sensitivity of  $< 3.1 \times 10^{-11}$  ergs/cm<sup>2</sup> sec in the 2-10 keV band. Of the 85 detected sources (excluding the LMC and SMC sources) 17 have been identified with galactic objects, 61 have been identified with extragalactic objects and 7 remain unidentified. The log N - log S relation for the non-galactic objects is well fit by the Euclidean relationship. We have used the X-ray spectra of these objects to construct log N - log S in physical units. The complete sample of identified sources has been used to construct X-ray luminosity functions, using the absolute maximum likelihood method, for clusters of galaxies and active galactic nuclei.

Keywords: X-Ray Sources, Luminosity Function, Cosmic X-Ray Background

<sup>1</sup>NAS/NRC Research Associate

<sup>2</sup>Also Dept. Physics & Astronomy, Univ. of Maryland

## I. INTRODUCTION

The HEAO-1 satellite experiment A-2 (Rothschild et al. 1979) with its extended energy range, complete sky coverage, low and stable internal background and moderate spatial resolution has enabled us to create a complete catalog of X-ray sources at galactic latitudes  $|b| > 20^\circ$  down to a limiting sensitivity of  $3.1 \times 10^{-11}$  ergs/cm<sup>2</sup> sec in the 2-10 keV band. Recent identifications of these sources by modulation collimator experiments on HEAO-1 and SAS-3 as well as imaging detectors on HEAO-2 has resulted in certain identifications of all sources of flux  $\geq 4.0 \times 10^{-11}$  ergs/cm<sup>2</sup> sec, pending confirmation of two clusters and NGC 7172, and reasonable identifications for 78 out of the 85 (92%) sources in the sample. All but 9 of these identifications are extremely likely or certain. This identification ratio for the extragalactic sources compares to identification of 45 out of 67 (67%) sources in the sample of Warwick and Pye (1979).

The completeness of this sample enables construction of the number-intensity distribution ( $\log N - \log S$ ) for X-ray sources as well as developing X-ray luminosity functions for clusters of galaxies and active galactic nuclei. In addition the body of X-ray spectral data returned by A-2 allows us to cast the  $\log N - \log S$  distribution in absolute rather than instrument dependent units which enables comparison with the  $\log N - \log S$  relation in different X-ray energy bands (cf. Giacconi et al. 1979).

Analysis of this data shows that the source counts are well fit by a "Euclidean" law with

$$\frac{dN}{dS} = 16.5 S^{-5/2} (\text{R15 cts/sec})^{-1} \text{sr}^{-1}$$

consistent with previous results despite the quite different samples (Warwick

and Pye 1978; Schwartz 1979). The luminosity functions are well fit by power law representations with

$$\frac{dN}{dL_{44}} \leq 3.5 \cdot 10^{-7} L_{44}^{-2.15} (10^{44} \text{ erg/sec})^{-1} \text{ Mpc}^{-3}$$

for clusters of galaxies, and

$$\frac{dN}{dL_{44}} \leq 2.7 \times 10^{-7} L_{44}^{-2.75} (10^{44} \text{ erg/sec})^{-1} \text{ Mpc}^{-3}$$

for active galactic nuclei, similar to previous results (McKee et al. 1980; Pye and Warwick 1979). Integration of the luminosity functions over the  $< 10^{42.5} - 10^{45}$  erg/sec range within which they are well determined results in estimates of the contribution of clusters and active galactic nuclei to the integral 2-10 keV unresolved X-ray background of  $\leq 4\%$  for clusters and  $\leq 20\%$  for active galaxies. Using these luminosity functions, with no evolution, we estimate that  $\leq 30\%$  of the sources seen in the Einstein Observatory deep survey (Giacconi et al. 1979) should be relatively low luminosity ( $L < 1 \times 10^{44}$  erg/sec) nearby ( $z \lesssim 0.5$ ) objects.

## II. DATA ANALYSIS AND SOURCE SELECTION

The HEAO-1 A-2 experiment, described in detail by Rothschild et al. (1979), provided two independent, low background, high sensitivity surveys of the entire sky six months apart. We have analyzed the A-2 data in order to obtain a complete flux limited sample of extragalactic X-ray sources. The region between  $-20^\circ$  and  $+20^\circ$  in galactic latitude has been excluded to minimize contamination from galactic sources. A circle of 6 degrees radius around the LMC sources has been also excluded to prevent confusion problems. Therefore, we remain with 65.5% of the sky (8.23 ster). The statistical

significance of the existence of the sources is tested by determining the decrease in  $\chi^2$  when the new source is added to the model. All sources in the sample give a decrease in  $\chi^2$  of at least 30. The probability of having, by chance, a decrease of 30 in  $\chi^2$  with two degrees of freedom (scan angle and intensity) is  $3 \times 10^{-7}$ . This probability is almost the same as the one associated with a deviation of  $5\sigma$  in a Gaussian distribution ( $6 \times 10^{-7}$ ). Therefore, we can also state that the lowest statistical significance for the existence of the sources included in our sample is  $5\sigma$ , as required by the maximum likelihood methods we use to determine the  $\log N - \log S$  parameters (see Section IV-1). Taking into account this statistical significance requirement we estimated the completeness level of the first and the second scan as 1.25 and 1.8 R15 counts/sec respectively, see Figure 1. One R15 count/sec  $\leq 2.17 \text{ erg cm}^{-2} \text{ sec}^{-1}$  in the 2-10 keV energy band for a power law spectrum with photon index 1.65. R15 is a counting rate derived using the  $1.5^\circ \times 3^\circ$  FWHM fields of view of the second layer of the argon counter and both layers of a xenon counter. This combination has a FWHM for the quantum efficiency from  $\sim 3$  to  $\sim 17$  keV (Marshall et al. 1979).

The second pass is less sensitive on average, because much more time was spent in pointing at sources. We shall be more concerned with the first pass data in deriving best fit parameters and use the second pass ones mostly as an independent confirmation.

### III. OBSERVATIONS

#### A. The Sample

Table 1 contains all the relevant data for the 68 sources either brighter than 1.25 R15 c/s in the first scan which corresponds to days 248-437 of 1977, or brighter than 1.8 in the second scan, days 73-254 of 1978. Source names are listed in column 1. Column 2 contains previous catalog names.

First pass fluxes and  $1\sigma$  errors are in column 3, while the second pass ones are in column 4. Some fluxes may differ slightly from previously reported results, as different procedures have been used; e.g., in the recent paper by McKee et al. (1980) fluxes have been obtained fixing the X-ray position at the optical position, instead here we have used the best fit X-ray position to derive the flux. Available identifications are listed in column 5. The type of object is in column 6. One \* in column 7 indicates firm identifications (i.e. as provided by the SAS-3 or HEAO-1 modulation collimators or by the Einstein X-ray telescope), two \* indicates possible identification consistent with larger error boxes. Redshift values and references are given in column 8. Spectral information is now available for more than half of our sources (Mushotzky et al. 1980; Worrall et al. 1980; Mushotzky 1979; Holt 1980; Boldt 1980), we quote in column 9 conversion factors between R15 counts/s and  $\text{ergs cm}^{-2} \text{s}^{-1}$ . When spectral information is lacking we assumed a 6 keV thermal bremsstrahlung spectrum for all sources identified with clusters and a 1.65 photon index power law for all sources identified with active galaxies. An average conversion factor value of  $2.5 \times 10^{-11} \text{ ergs cm}^{-2} \text{ s}^{-1}/\text{R15 counts s}^{-1}$  was assumed for the few unidentified sources. Columns 10 and 11 contain the first and second pass luminosities in units of  $10^{44} \text{ erg s}^{-1}$  calculated for  $H_0 = 50 \text{ km/s/Mpc}$  and  $q_0 = 0.5$ . Column 12 contains notes.

#### B. Classes of Sources

Sixty of the 82 sources brighter than  $1.25 \text{ counts s}^{-1}$  in the first scan and not definitely associated with galactic objects have been associated with extragalactic objects. Only 7 remain unidentified at the present time. These 60 identified sources subdivide almost equally between clusters of galaxies (30) and single galaxies (30). Most of the 30 galaxies are Seyfert galaxies of class 1 or 2, but we have also 1 QSO (3C 273), 4 BL Lac objects, and 1



"normal" galaxy (NGC 7172). Note that M31 and the Magellanic Cloud sources are not included in our extragalactic sample because they represent a local inhomogeneity as part of the local group of galaxies. Table 2 lists the 17 high galactic latitude sources not included in our extragalactic sample because they have been identified with galactic or "local" objects. The second pass sample contains only 37 sources brighter than 1.8 R15 counts/sec, all but one identified. The source classification is consistent with the first pass. Assuming Poisson errors, clusters contribute  $50 \pm 9\%$  of the identified sources in the first pass and  $61 \pm 13\%$  in the second. Galaxies contribute  $50 \pm 9\%$  in the first scan and  $39 \pm 10\%$  in the second.

#### C. New Sources and Sample Completeness

H0328+025 and H0917-075 are the only entirely new sources in Table 1. Figure 2 shows their error boxes. All the other sources in Table 1 have been listed somewhere else before. The improvement in our sample, as compared to previously reported ones, is due to a better rejection of non-extragalactic sources, made possible by the recent identifications, and to a uniform sky coverage to a relatively low limiting flux.

As the instrument has a fairly large ( $1.5^\circ \times 3.0^\circ$ ) angular resolution the possibility of source confusion must be considered. The total area of the sky included in this survey is approximately  $2.7 \times 10^4$  square degrees, therefore there are about  $6 \times 10^3$  independent positions on it. As the high galactic latitude X-ray sources bright enough to give confusion problems at our sensitivity level cannot be more than a hundred using the log N-log S relation derived later (taking into account also the possibility that two weaker sources can simulate a source bright enough to be included in our list) we therefore expect negligible confusion. That is using  $\frac{dN}{dS} < 16.5 S^{-1.5}$  there are roughly 65 resolution elements per source, of  $S > 1.25$  cts, well above the

confusion level of 25 beam areas per source often quoted in the literature. In addition the uniform sky coverage at the chosen sensitivity levels provided by this experiment and the availability of two independent sets of data for cross-checking purposes support our confidence in the completeness of our sample.

#### D. Space Distribution of Sources

Since the pioneering work of DeVaucouleurs (1958) much attention has been devoted to finding evidence of a supercluster centered in the Virgo cluster of galaxies. We plotted the positions of our sources in supergalactic coordinates looking for some kind of anisotropy. Figure 3 shows the 1st pass sample. Obviously, no anisotropy is observed as most sources lie beyond the supercluster. If we restrict our attention to the 12 sources with redshifts less than .01 (in boxes in Figure 3), we see that 9 are in the center region of the supercluster while 3 are in the anticenter and that all but one have supergalactic latitude less than 30 degrees in absolute value. This result, which is significant at the few percent level, suggests that close X-ray galaxies may lie preferentially in the supergalactic plane. But no conclusion can safely be made from such a small number of objects at present.

### IV. THE NUMBER-FLUX FUNCTION

The usual power law form

$$N(S) = KS^{-\alpha} \quad (\text{R15 counts/sec})^{-1} \text{sr}^{-1} \quad (1)$$

has been assumed for the number-flux relation. The various methods applied to estimate the coefficient K and the differential exponent  $\alpha$  as well as to evaluate the goodness of the fit are outlined in the next section.

#### A. Statistical Methods

## 1. Maximum Likelihood

Crawford, Jauncey and Murdoch applied the maximum likelihood method to unbinned data in order to estimate the slope of the number-flux relation of radio sources. In the first paper (Crawford et al. (1970) a solution is worked out for error free data. In the second paper (Murdoch et al. 1973) the method is extended to include errors on the measured fluxes. Numerical corrections to the error free answers were calculated for the special case of Gaussian distributed errors. In the same paper it was pointed out that a minimum signal-to-noise ratio of five is required so that the uncertainty in the correction factor due to weaker sources does not dominate the correction itself. This is why we excluded from our sample sources with statistical significance less than  $5\sigma$ . In both Papers I and II the Kolmogorov-Smirnov test (here after: K-S test) was suggested to evaluate the goodness of the fit obtained. In the remainder of this paper we will refer to this method as to the Maximum Likelihood (ML) method.

## 2. Absolute Maximum Likelihood

The ML method assumes the same underlying error distribution for all the sources in the sample, i.e. it assigns the same  $1\sigma$  error to all the sources. As we deal with sources of greater than  $5\sigma$  significance the error assumed is one fifth of the minimum flux in the sample, or  $.25 R_{15} \text{ counts s}^{-1}$  in the first scan and  $.36 R_{15} \text{ counts s}^{-1}$  in the second. Table 1 shows that these values are not very far from the actual errors. However Lightman et al. (1980) have developed a refinement of the ML method in connection with the K-S test capable of handling sources with their own experimental error. Following those authors we will call this new statistical method the "Absolute Maximum Likelihood" (AML) method. Lightman et al. (1980) worked out the AML method on general grounds and then applied it to the evaluation of globular cluster

X-ray source masses. As this is the first application of the AML method to the number flux function, we give a short outline of the method below.

Assuming the form (1) for the number-flux relation and a Gaussian form  $\rho(F_i, \sigma_i, S)$  for the error distribution of the measured fluxes we evaluated numerically the integral probabilities  $\hat{P}_i(\alpha)$  as

$$\hat{P}_i(\alpha) = \frac{\int_{F_{\min}}^{F_i} dF \int_{F_{CO}}^{\infty} dS N(S, \alpha) \rho(F, \sigma_i, S)}{\int_{F_{\min}}^{\infty} dF \int_{F_{CO}}^{\infty} dS N(S, \alpha) \rho(F, \sigma_i, S)} \quad (2)$$

where  $S$  is the true flux,  $F_i$  and  $\sigma_i$  are the measured flux and error of the  $i$ -th source.  $F_{CO}$  is a cutoff value used to avoid the apparent divergence at  $F = 0$ . As in Murdoch et al. (1973) the particular choice of the cutoff value does not affect the value of the integral as long as the statistical significance of the sources is at least  $5\sigma$ .  $F_{\min}$  is the sensitivity limit of the sample. For every assumed  $\alpha$  we computed the  $\hat{P}_i(\alpha)$  for all the sources. The  $\hat{P}_i(\alpha)$  should be uniformly distributed between 0 and 1. Following Lightman et al. we evaluated the maximum deviation from the uniform distribution:

$$D_{\max}(\alpha) = \max_{i=1, N} [D_i(\alpha)] = \max_{i=1, N} \left( \left| \hat{P}_i(\alpha) - \frac{i}{N} \right| \right) \quad (3)$$

where  $N$  is the number of sources in the sample and the  $\hat{P}_i(\alpha)$  have been sorted in ascending order. Then we calculate the probability  $P(D_{\max}(\alpha))$  of observing deviations greater than  $D_{\max}(\alpha)$  from the formula for the K-S statistic given by Birnbaum and Tingey (1951). The  $(\alpha, P(D_{\max}(\alpha)))$  function is then plotted. The best fit value of  $\alpha$  is the one corresponding to the maximum

value  $P_{\text{MAX}}$  of the  $P(D_{\text{max}}(\alpha))$  distribution. Obviously  $P_{\text{MAX}}$  must be greater than some minimum value (say 10%) in order to accept the model. The range in  $\alpha$  for results given below on  $\alpha$  are evaluated from the values  $\alpha_1$  and  $\alpha_2$  of  $\alpha$ , which reduce  $P(D_{\text{max}}(\alpha))$  to  $P_{\text{MAX}}/2$ .

### 3. Chi-Square

Both the ML and the AML methods are independent of the coefficient  $\kappa$  of the number-flux relation, as  $\kappa$  is lost in normalizing the probabilities. Therefore, we used the  $\chi^2$  method to determine  $\kappa$ . Bins with equal expected number of sources for  $\alpha = 2.5$  have been used for the  $\chi^2$  calculations. Of course, in calculating confidence bounds, we have assumed that the functional form of the distribution is the "true" one. If better data later shows that this is not true our confidence values are not applicable.

### V. LOG N - LOG S RESULTS

The ML method applied to the 60 non-galactic sources brighter than 1.25 R15 counts  $s^{-1}$  in the first pass gives (in this section we use R15 counts  $s^{-1}$  as the unit)

$$\alpha = 2.67 \pm .23$$

with a goodness of fit probability (evaluated using the KS test) of 39.5 percent.

For the 37 non-galactic sources brighter than 1.8 R15 counts  $s^{-1}$  in the second pass the ML result is

$$\alpha = 2.74 \pm .32$$

with a probability of 17.5 percent.

The AML results are

$$\alpha = 2.63 \pm .2$$

in the first pass, see Figure 4a, and

$$\alpha = 2.74 \pm .22$$

in the second, see Figure 4b.

The 68 and 95 percent probability contours for the 1st pass values of  $\kappa$  and  $\alpha$  evaluated with the  $\chi^2$  method are plotted in Figure 4c. The  $\chi^2$  best fit values and 1 $\sigma$  errors for the number-flux function parameters are

$$\alpha = 2.72^{-.10}_{+.15} \quad (4)$$

$$\kappa = 20^{-.2.6}_{+4.0} \text{ (R15 counts/sec)}^{\alpha-1} \text{ sr}^{-1}.$$

The differential number-flux data as well as the best fit function

$$N(S) = 20 S^{-2.72} \text{ (R15 counts/sec)}^{-1} \text{ sr}^{-1}$$

are plotted in Figure 5; the  $\chi^2$  value of the fit is 2.79 for 6 degrees of freedom, corresponding to a probability  $P(> \chi^2) \leq 83\%$ . The limited size of the second scan sample does not allow a good estimate of the probability but the results are consistent with the first pass ones.

### C. Number Flux Relation in Physical Units

Using the conversions factors listed in column (9) of Table 1 we can

express the fluxes in  $\text{ergs cm}^{-2} \text{s}^{-1}$  and evaluate the number-flux relation accordingly. Conversion factors range approximately from  $2.0 \times 10^{-11}$  to  $2.9 \times 10^{-11} \text{ ergs cm}^{-2} \text{s}^{-1} (\text{R15 counts s}^{-1})^{-1}$ , the highest values referring to soft spectra sources whose emission peak lies below our instrument energy window. As a consequence of the different conversions factors the completeness level of the samples when fluxes are in  $\text{ergs cm}^{-2} \text{s}^{-1}$  is equal to the former completeness level in  $\text{R15 counts s}^{-1}$  times the maximum conversion factor: that is  $< 3.6 \times 10^{-11} \text{ ergs cm}^{-2} \text{s}^{-1}$  for the first pass and  $5.2 \times 10^{-11} \text{ ergs/cm}^2 \text{ sec}$  in the second pass. The 1st scan sample with this flux restriction contains 51 sources: 25 clusters, 22 "galaxies" and 4 unidentified sources. The best fit values and  $1 \sigma$  errors for the number-flux function parameters obtained with the three methods agree with

$$\begin{aligned} \alpha &\leq 2.85 \pm .3 \\ \kappa &\leq (5.65_{-1.3}^{+1.9}) \times 10^{-19} (\text{ergs cm}^{-2} \text{s}^{-1})^{\alpha-1} \text{sr}^{-1} \end{aligned} \quad (5)$$

The 32 second scan sources brighter than  $5.2 \times 10^{-11} \text{ ergs cm}^{-2} \text{s}^{-1}$  give us a best fit of slightly steeper slope  $\alpha \leq 3.1 \pm .4$ .

## VI. DISCUSSION OF THE RESULTS

All the first pass samples, whether fluxes are expressed in R15 counts  $\text{s}^{-1}$  or in  $\text{ergs cm}^{-2} \text{s}^{-1}$  are consistent with the five halves Euclidean slope (see Figures 6 and 7). The slight preference for a steeper than Euclidean slope is due to the distribution of the brightest few sources in calculating the likelihood functions. It is these sources that are most sensitive to changes in  $\alpha$  by virtue of the relatively small statistical error in their measured intensity. Our Euclidean best fit for the 1st pass data is

$$N(S) = 16.5_{-2}^{+3} S^{-2.5} (\text{R15 counts/s})^{-1} \text{sr}^{-1}$$

with a  $\chi^2$  of 5.5 for 7 degrees of freedom;  $p(\chi^2 > 5.5) \leq 60\%$ . The AML probability for  $\alpha = 2.5$  is 42.4%. Assuming an average conversion factor of  $2.4 \times 10^{-11}$  ergs  $\text{cm}^{-2} \text{s}^{-1}$  (R15 counts  $\text{s}^{-1}$ ) the relation (4) becomes

$$N(S) \leq (1.9_{-.25}^{+.35}) \times 10^{-15} S^{-2.5} (\text{ergs cm}^{-2} \text{s}^{-1})^{-1} \text{sr}^{-1}$$

in agreement with the exact result

$$N(S) \leq (2.2_{-.2}^{+.3}) \times 10^{-15} S^{-2.5} (\text{ergs cm}^{-2} \text{s}^{-1})^{-1} \text{sr}^{-1}$$

obtained from the 1st pass complete sample for fluxes in ergs  $\text{cm}^{-2} \text{s}^{-1}$  and using the conversion factors in Table 1.

#### VII. COMPARISON WITH PREVIOUS EXPERIMENTS

Both the Uhuru (Schwartz 1979) and Ariel 5 data (Warwick and Pye 1978) gave a flux-number function consistent with the Euclidean model. Their best fit values for the coefficient  $\kappa$  with  $\alpha = 2.5$  and  $S$  in R15 counts  $\text{s}^{-1}$  are respectively

$$\kappa = 16.5 \pm 3.9 \quad \text{using } 1 \text{ Uhuru ct/s} = 1.0 \text{ R15 ct/sec}$$

and

$$\kappa = 15.8 \pm 4.2 \quad \text{using } 1 \text{ Ariel-5 ct/sec} = 2.12 \text{ R15 ct/sec}$$

in agreement with our results at the  $1\sigma$  level. These conversion factors assume a mean R15 conversion factor of  $2.4 \times 10^{-11}$  ergs/sec, 1 Uhuru ct/sec =  $2.4 \times 10^{-11}$  erg/sec, and 1 Ariel-5 count/sec =  $5.1 \times 10^{-11}$  erg/sec. If we use the calibration of Marshall et al. (1979) appropriate for the active galaxies of 1 R15 ct/sec =  $2.17 \times 10^{-11}$  erg/cm<sup>2</sup> sec, we find  $\kappa_{\text{Uhuru}} < 20$  and



<sup>K</sup>Ariel-5  $\leq 19$ . The best fit slope of Warwick and Pye of  $2.7 \pm .2$  is also consistent with our result.

### VIII. LUMINOSITY FUNCTION

#### A. Method and Data Base

Many authors (Schwartz 1978; McHardy 1978; McKee et al. 1980; Elvis et al. 1977; Pye and Warwick 1979; Tananbaum et al. 1978; Boldt 1980) have recently considered the problem of evaluating the X-ray luminosity functions for different classes of sources principally, clusters of galaxies and active galaxies. All of them with the exception of Pye and Warwick had to rely upon optical data to select complete samples. We present here X-ray luminosity functions evaluated from X-ray flux limited samples. As we remain with a few unidentified sources, our results have some uncertainty, but we believe that the residual incompleteness should not be very important.

#### 1. The Samples

The first pass sample of clusters of galaxies contains 30 objects. The second pass one includes 22 sources. Thirty "galaxies" are observed in the first pass, but we exclude from our sample the QSO 3C273, the 4 BL Lac objects, the peculiar galaxy M82 and the "normal" galaxy NGC 7172 as they are not homogeneous with the bulk of the sample which consists of Seyfert galaxies. Therefore we remain with 23 active galactic nuclei. The second pass sample contains only 12 objects (after excluding 3C 273 and PKS 2155-304).

The completeness of the sample is checked using the Schmidt  $\langle V/V_M \rangle$  test and with a K-S test on the distribution of the  $V_i/V_{M_i}$  as suggested by Avni and Bahcall (1980). The results are listed in Table 3.

TABLE 3

<u>CLASS OF OBJECTS</u>	<u>SCAN #</u>	<u># OBJECTS</u>		<u>K-S TEST</u>
		<u>IN SAMPLE</u>	<u>&lt;V/V<sub>M</sub>&gt;</u>	<u>P(&gt;d) %</u>
Clusters of Galaxies	1	30	.471±.054	18.1
Clusters of Galaxies	2	22	.552±.062	11.8
Active Galaxies	1	24	.523±.059	50.4
Active Galaxies	2	12	.557±.083	56.8

The  $1\sigma$  error quoted for  $\langle V/V_M \rangle$  is the formal error  $1/\sqrt{12N}$ , where  $N$  is the number of objects in the sample (see Avni and Bahcall). All the 4 samples meet the requirements of the tests. However, we expect a small degree of incompleteness due to the unidentified sources.

## 2. Methods of Analysis

Of the three methods outlined in Sec (IV-A) only the AML is suited for the determination of the luminosity function parameters. The relatively small sizes of the samples do not allow an efficient use of the  $\chi^2$  square method or of any other binned method. Moreover the ML method in the form developed by Crawford, Jauncy and Murdoch cannot be used because of its assumptions of a single underlying error distribution. This last hypothesis was reasonably satisfied by the flux data in the evaluation of the  $\log N \log S$  parameters, as we already pointed out, but is not satisfied at all by the luminosity data, as the errors are proportional to the square of the redshift of the sources:

$$\sigma_{L_i} \approx z_i^2 \sigma_{F_i} \quad (6)$$

On the contrary the AML method is well suited for the task. The description of Section IV-A still applies. However, instead of calculating the probabilities of eq (2) we evaluated the probabilities:

$$P_i(q) = \frac{\int_0^{L_i} dL' \int_{L_{\min}}^{L_{\max}} dL f(L,q) V_{\max}(L, F_{\min}) \rho(L, \sigma_{L_i}, L)}{\int_0^{\infty} dL' \int_{L_{\min}}^{L_{\max}} dL f(L,q) V_{\max}(L, F_{\min}) \rho(L, \sigma_{L_i}, L)} \quad (7)$$

Eq. (7) gives the integral normalized probabilities of observing a source with measured luminosity less or equal to  $L_i$ , assuming a Gaussian error distribution with standard deviation  $\sigma_{L_i}$ , and for the differential luminosity function the form  $f(L,q)$  where  $L$  is the true luminosity and  $q$  represents the functional parameters to be determined.  $L_{\min}$  and  $L_{\max}$  are the lower and upper boundaries of the luminosity function.  $V_{\max}$  is the maximum volume at which one could detect the source and depends on the sensitivity limit of the sample. For a source of luminosity  $L$  in a sample of minimum sensitivity  $F_{\min}$  the maximum visibility volume  $V_{\max}$  is proportional to

$(\sqrt{L/F_{\min}})^3$  Note that Eq. (7) does not take in account errors on the redshift

$z$ . The AML method can determine the form of the luminosity function but not its absolute value. Therefore we have used a least squares fit to the unbinned data to evaluate the multiplicative coefficient.

## B. Results

### 1. Clusters of Galaxies Luminosity Function

We considered two different forms for the luminosity function: the power law form

$$f(L) = KL^{-\gamma}$$

and the exponential form

$$f(L) = Ke^{-L/L_0}$$

between the minimum ( $L_{44\text{min}}$ ) and maximum ( $L_{44\text{max}}$ ) observed luminosities, expressed in units of  $10^{44}$  ergs  $\text{sec}^{-1}$ . The normalization for a power law luminosity function scales as  $H_0^{-1}$ .

#### Clusters of Galaxies

Figure 9 represents the AML probabilities for the slope of the cluster of galaxies power law luminosity function. The 1st pass best fit values for the power law parameters are

$$\gamma = 2.15^{+0.12}_{-0.17}$$

$$K = (3.5 \pm 1.1) \times 10^{-7} (10^{44} \text{ erg/s})^{\gamma-1} \text{ Mpc}^{-3}.$$

K has been evaluated with the least squares method. The error on K has been determined by letting  $\gamma$  assume the  $1\sigma$  extreme values of 2.03 and 2.32. Figure 8a gives a binned representation of the data with the best fit luminosity function. Each bin contains three sources, except for the highest luminosity bin which contains five. The second pass results are

$$\gamma = 2.13^{+0.16}_{-0.24}$$

$$K = (3.8 \pm 2) \times 10^{-7} (10^{44} \text{ ergs/s})^{\gamma-1} \text{ Mpc}^{-3}$$

Figure 8b give the binned representation. The minimum luminosity object in both the 1st and the 2nd pass at  $2.4 \times 10^{43}$  (ergs/s) is the Virgo cluster. The highest luminosity cluster is Abell 2142 with  $2.8 \times 10^{45}$  (ergs/s).

The exponential form of the luminosity function has also been considered, but the quality of the fit is poorer, see Figure 10.

As the Virgo Cluster of galaxies has a "local" character, we evaluated the cluster of galaxies luminosity function without the Virgo cluster. The 1st pass sample is reduced to 29 sources, the mean  $V/V_{MAX}$  is  $0.486 \pm 0.055$  and the K-S test on the uniformity of the  $V/V_{MAX}$  distribution gives a probability of 24.7%. The 2nd pass sample contains 21 sources, the mean  $V/V_{MAX}$  is  $0.576 \pm .063$  and the K-S probability is 6.1%. Figure 9 gives the usual  $(\gamma, P(\gamma))$  probability curves for the power law slope. The best fit values for the parameters are

$$\begin{aligned} \text{1st scan} \quad \gamma &= 2.03 \pm .18 \\ K &= (2_{-.8}^{+1.2}) \times 10^{-7} (10^{44} \text{ ergs/s})^{\gamma-1} \text{ Mpc}^{-3} \end{aligned}$$

$$\begin{aligned} \text{2nd scan} \quad \gamma &= 2.07_{-.25}^{+.2} \\ K &= (3.2 \pm 2) \times 10^{-7} (10^{44} \text{ ergs/s})^{\gamma-1} \text{ Mpc}^{-3}. \end{aligned}$$

The minimum luminosity is now  $\leq 3.6 \times 10^{43}$  ergs/s (Abell 1060) in both first and second scan. The exponential fit is again poorer, see Figure 10.

## 2. Active Galaxies

### i. Luminosity Function

The insert in Figure 11 represents the AML probability for the power law slope of the active galaxies differential luminosity function calculated from the 1st pass data. The best fit values for the power law parameters are:

$$\begin{aligned} \gamma &= 2.75 \pm .15 \\ K &= (2.7 \pm .15) \times 10^{-7} (10^{44} \text{ ergs/s})^{\gamma-1} \text{ Mpc}^{-3}. \end{aligned}$$

NGC 3227 is the weakest source in the sample with  $1.75 \times 10^{42}$  ergs/s and

III Zw2 is the brightest with  $1.3 \times 10^{45}$  ergs/s. Figure 11 shows the binned representation (3 sources/bin). This result is similar to that of Boldt (1980) and Pye and Warwick (1979). The exponential form for the luminosity function is not acceptable as the probabilities are always less than 2%.

The second pass sample is too small for a good determination of the luminosity function, however we find power law slopes steeper but consistent with the first pass ones

ii. A Lower Limit to the Active Galaxy Luminosity Function

The active galaxies contribution to the cosmic X-ray background depends strongly on the lower luminosity limit of the luminosity function. The lower luminosity limit for which the function can represent the data,  $L_{44\text{MIN}}$ , can be calculated by noting that the luminosity function must be consistent with the log N - log S observations. Namely, we can set a lower limit on  $L_{44\text{MIN}}$  by requiring that the number of active galaxies brighter than 1.25 R15 counts/sec expected from the luminosity function does not exceed the observed number plus 1 or 2 times the square root of the expected number.

From eq (14.7.35) of Weinberg (1972), and assuming a power law luminosity function we have (for  $\gamma \neq 2.5$  and  $\gamma \neq 3$ )

$$N(>S) \approx KA \left[ \frac{1}{2.5-\gamma} \left[ L^{2.5-\gamma} \right]_{L_{\text{MIN}}}^{L_{\text{MAX}}} S^{-3/2} - \frac{B}{3-\gamma} \left[ L^{3-\gamma} \right]_{L_{\text{MIN}}}^{L_{\text{MAX}}} S^{-2} \right] \quad (8)$$

where: S is the flux in  $\text{ergs cm}^{-2}\text{s}^{-1}$

K and  $\gamma$  are the parameters of the differential power law luminosity function in  $\text{Mpc}^{-3} (\text{erg/sec})^{-(\gamma-1)}$

$L_{\text{MAX}}$  and  $L_{\text{MIN}}$  are the upper and lower limit of the luminosity function (actually  $N(>S)$  depends strongly on  $L_{\text{MIN}}$  and very weakly on  $L_{\text{MAX}}$ )

all the luminosities are in ergs/s

$$A \approx 3.20 \times 10^{-75}$$

$$B \approx 4.7 \times 10^{-29} \text{ (assuming } H_0 = 50 \text{ km/s/Mpc)}$$

$N(>S)$  is the total number of sources in the sky uncorrected

for sky coverage. The second term of this equation represents a first order cosmological correction to the Euclidian result. (1)

.....

(1) Footnote:

For  $L$  in units of  $10^{44}$  erg/sec equation (8) has constants

$$A = 3.2 \times 10^{-9}$$

$B = 2.3 \times 10^{-7} (H_0/50) (1+\Gamma)$  where  $\Gamma$  is the spectral index of the source (here chosen to be .7)

.....

Assuming an average conversion factor of  $2.17 \times 10^{-11}$  ergs  $\text{cm}^{-2}\text{s}^{-1}$  per R15 counts  $\text{s}^{-1}$  we find that the  $1\sigma$  lower limit on  $L_{\text{MIN}}$  is  $4 \times 10^{42}$  when  $\gamma$  is 2.75 and  $K$  is  $2.68 \times 10^{-7} (10^{44} \text{ ergs/s})^{-1} \text{ Mpc}^{-3}$  and  $L_{\text{MAX}}$  varies between 5 and  $15 \times 10^{44}$  ergs/sec.

In Table 4 we show the  $1$  and  $2\sigma$  limits on  $L_{\text{MIN}}$  as a function of  $L_{\text{MAX}}$  and  $\gamma$ . We note that we have not included in Table 4 the possibility that all (or some) of the unidentified sources could be Seyfert galaxies. However, considering the distribution of identified sources with flux  $< 3$  R15 cts/sec, we would expect, at most, 3 of these unidentified objects to be active galaxies.

TABLE 4

APPROXIMATE  $L_{\text{MIN}}$  FOR VALUES OF  $L_{\text{MAX}}$  AND  $\gamma$

$$L_{\text{MAX}} = 1.5 \times 10^{45}$$

$$L_{\text{MAX}} = 3 \times 10^{45}$$

	Y			Y		
	2.6	2.75	2.9	2.6	2.75	2.9
1 $\sigma$	1.5x10 <sup>42</sup>	2.5x10 <sup>42</sup>	4.5x10 <sup>42</sup>	1.5x10 <sup>42</sup>	3.0x10 <sup>42</sup>	4.5x10 <sup>42</sup>
2 $\sigma$	4.5x10 <sup>41</sup>	1.5x10 <sup>42</sup>	2.5x10 <sup>42</sup>	5.5x10 <sup>41</sup>	1.5x10 <sup>42</sup>	3.0x10 <sup>42</sup>

### C. Discussion

#### 1. Clusters of Galaxies

We note that our luminosity function for clusters of galaxies is very similar to the result of McKee et al. (1980). This indicates that, whatever selection effects are operating in making a X-ray or optically complete sample, they do not strongly bias the result. However there is a strong overlap in the individual objects between this sample and McKee's. The method we have used has allowed us in principle to discriminate between exponential and power law luminosity functions for clusters. It is somewhat surprising that a power law is favored, since it requires a change in form at low luminosities in order not to exceed the space density of all clusters (Bahcall 1979). However, the contribution of clusters to the diffuse X-ray background (DXRB) depends only weakly on the lower limit chosen. We do remind the reader that an exponential form is not excluded. Our data are not capable of rejecting the exponential form. They are also not capable of determining well the three constants in Bahcall's (1979) suggested form of the luminosity function.

Keeping in mind that the mean X-ray spectrum of clusters differs significantly from the diffuse X-ray background we shall, for historical reasons, compare the 2-10 keV volume emissivity of clusters to that of the diffuse X-ray background. For  $q_0 = 1/2$ ,  $H_0 = 50$  km/sec/Mpc the 2-10 keV background has a volume emissivity of  $\leq 2.4 \times 10^{39}$  erg/sec/Mpc<sup>3</sup>. The



contribution of clusters is

$$\int_{L_{\text{MAX}}}^{L_{\text{MIN}}} f(L) L dL \leq 1 \times 10^{38} \text{ ergs/sec/Mpc}^3$$

(for  $L_{\text{MAX}} = 3 \times 10^{45}$  ergs/sec,  $L_{\text{MIN}} = 1 \times 10^{43}$  ergs/sec, where we have used the 1st pass cluster power law luminosity function without the Virgo cluster). Therefore, in an average sense, clusters contribute  $\leq 4\%$  of the 2-10 keV background. (For a more accurate treatment of the problem which includes the effect of the spectral differences of clusters from the background see McKee et al. 1980 and Marshall et al. 1980). We note that the present value agrees well with the estimate made by Marshall et al. (1980) of the maximum possible contribution of clusters if they were not to distort the thermal bremsstrahlung fit to the spectrum of the DXRB in the 3-50 keV band. We note that the relatively soft spectra of clusters should result in an increase in their contribution to the DXRB in the Einstein Observatory energy range.

## 2. Active Galaxies

The luminosity function derived here is in reasonable agreement with those derived previously by Pye and Warwick (1979) and Boldt (1980) in both slope and normalization. Using a lower bound of  $3.0 \times 10^{42}$  ergs/sec and an upper bound of  $1.5 \times 10^{45}$  erg/sec for our luminosity function results in a volume emissivity of  $\leq 4.9 \times 10^{38}$  ergs/sec Mpc<sup>3</sup> or a contribution of  $\leq 20\%$  to the 2-10 keV DXRB. If the lower limit is  $1.2 \times 10^{42}$  (see Table 4) the contribution to the DXRB is  $\leq 40\%$ . In fact, in order not to exceed the DXRB the luminosity function of AGN's must flatten at  $L \geq 3 \times 10^{41}$  ergs/sec (De Zotti 1980). There is a strong indication of such a flattening in the optical luminosity function (Huchra and Sargent 1973; Huchra 1977; Huchra 1980) at

$M_V \leq -21.5$  ( $H_0 = 50$ ) equivalent to a optical bolometric luminosity of  $\leq 1.2 \times 10^{44}$  ergs/sec. Since the slope of the optical luminosity function, at higher luminosities, is the same, within errors, (Huchra and Sargent 1973; Weedman 1979) as the X-ray function it is tempting to associate the bend in the optical luminosity function with the bend in the X-ray function and therefore derive a  $L_{\text{opt}}/L_X \leq 35$ . This value is rather larger than that found by examining individual objects (Kriss et al. 1980; Elvis et al 1978). This may be due to the fact that most of the optical flux from low luminosity active galaxies does not come from the nucleus but from the stellar population.

The total space density of X-ray emitting active galaxies in the luminosity range  $3 \times 10^{42} - 1.5 \times 10^{45}$  is  $\leq 7 \times 10^{-5} \text{ Mpc}^{-3}$  which is  $\leq 1.5\%$  of all galaxies of  $M_p < -19$  (Huchra 1977). This compares to a space density of active galaxies of  $M_p < -19$  of  $\leq 5 \times 10^{-5} \text{ Mpc}^{-3}$  (Huchra 1977, 1980). It thus seems, to first order, that all active galaxies of  $M_p < -19$  emit X-rays at  $L_X > 3 \times 10^{42}$  ergs/sec. For a flat universe there are (assuming no evolution)  $\leq 4 \times 10^7$  X-ray emitting active galaxies with  $L_X > 3 \times 10^{42}$  with  $z \leq 3.5$ .

We can also estimate, the number of sources per square degree expected in the Einstein deep survey if the luminosity function used in this paper does not evolve strongly in either slope or norm and that spectral effects, such as low energy absorption, are not important. With  $q_0 = .5$ ,  $L_{\text{min}} = 3 \times 10^{42}$  in the 2-10 keV band and,  $S_{\text{min}} = 5 \times 10^{-14}$  ergs/cm<sup>2</sup>sec in the 2-10 keV band, (which corresponds to the Einstein "deep survey" limit for a  $\alpha = 0.7$  source we predict  $\leq 6$  active galaxies per square degree and  $\leq 1.3$  clusters per square degree, compared to the  $19 \pm 8$  total sources per square degree seen by the Einstein Observatory (Giacconi et al. 1979). DeZotti (1980) has performed a similar calculation and finds  $\leq 5$  active galaxies per square degree for  $L_{\text{min}} =$

$9.1 \times 10^{41}$  and  $L_{\max} = 2.9 \times 10^{44}$  ergs/sec in the 2-6 keV band and assuming that the slope of the luminosity function is 2.5. Since most of the objects are near  $L_{\min}$  we would expect many of the Einstein survey objects to be Seyfert galaxies of  $L_x \lesssim 5 \times 10^{42}$  erg/sec and  $z \lesssim .20$ . This is a consequence of the well known fact that if the luminosity function is steeper than 2.5, and barring strong evolution, when one looks at fainter objects one is looking primarily lower in the luminosity function rather than at higher redshift objects.

A simple way to look at the problem is to examine the number of objects predicted by our best fit luminosity function which would have redshifts  $(z) \lesssim 0.5$  and would have luminosities high enough to have been included in the Einstein Deep Survey. (We shall use  $q_0 = .5$  or 0 geometry for simplicity). For  $S_{\min} = 5 \times 10^{-14}$  ergs/cm<sup>2</sup> sec in the 2-10 keV band and  $q_0 = .5$  that we predict  $\lesssim 1.4 \times 10^4$  sources/ster due to active galaxies and  $\lesssim 1.4 \times 10^3$  sources/ster due to clusters compared to the  $6.3 \pm 2.6 \times 10^4$  sources/ster seen in the deep survey (Giacconi et al. 1979). We therefore predict that  $\lesssim 25\%_{-8}^{+17}$

of the sources in the deep survey are low ( $L \lesssim 4 \times 10^{43}$ ) close by ( $z \lesssim .5$ ) active galaxies or clusters of galaxies of luminosity  $> 1 \times 10^{43}$  erg/sec. That this was a likely situation was noted by Fabian and Rees (1978). (If  $q_0 = 0$  the number of sources increases to  $\lesssim 2.1 \times 10^4$  sources/ster and the calculated contribution to the Einstein source counts to  $35_{-11}^{+24}\%$ ).

Both the contribution of active galaxies to the DXRB and their contribution to the Einstein source counts depend sensitively on the lower limit,  $L_{\min}$ , of the luminosity function used. It is possible that the luminosity where the flattening of the luminosity function takes place could be higher than our calculated value if we allow a two slope model of the luminosity function rather than our simple single slope power law model with a

cutoff. However our data are not good enough to constrain such a model. We therefore strongly caution the reader that these results are model dependant and should be treated as such.

#### IX. CONCLUSIONS

We have performed an all sky survey of X-ray sources complete to a limiting sensitivity of  $3.1 \times 10^{-11}$  ergs/cm<sup>2</sup> sec in the 2-10 keV band. Of the 85 detected sources only 7 remain without reasonable identifications. The log N- log S relation for extragalactic sources is well fit by a Euclidean law  $\frac{dN}{dS} = 16.5 S^{-2.5}$  where S is in R15 ct/sec or  $\frac{dN}{dS} = 2.2 \times 10^{-15} S^{-2.5} (\text{erg/cm}^2\text{s})^{-1} \text{sr}^{-1}$  where S is in erg/cm<sup>2</sup>s in the 2-10 keV band. This complete sample has allowed construction of luminosity functions based on a flux limited sample for clusters of galaxies and active galactic nuclei. These functions are well represented by power laws of slope 2.05 and 2.75 respectively. The sample enables us to estimate that the luminosity function for active galaxies should flatten at  $L \lesssim 3 \times 10^{42}$  erg/sec in the 2-10 keV band. The space density of X-ray emitting active galaxies is approximately the same as that of optically selected Seyfert galaxies.

Integration of the best fit luminosity functions indicates that clusters of galaxies contribute  $\lesssim 4\%$  of the 2-10 keV diffuse X-ray background and active galactic nuclei  $\lesssim 20\%$ . The sum of these contributions is very similar to the  $26 \pm 11\%$  contribution due to resolved sources seen in the Einstein deep survey. We also predict that many of the objects seen in the deep survey should be local, ( $z < 0.5$ ), relatively low luminosity active galactic nuclei and clusters of galaxies. In order to determine more accurately the contribution of low luminosity active galaxies to the diffuse X-ray background one would have to sample the luminosity range  $10^{41-42.5}$  over large solid angles. This would require a complete sky survey with  $\lesssim 30$  times the

sensitivity of the present one and a angular resolution  $\leq 20$  times better. Such a survey would also extend the luminosity function up to luminosities of  $\leq 10^{47}$  ergs/sec. We stress the importance of a complete unbiased X-ray survey with good identifications in determining  $\log N - \log S$  and luminosity functions since there are various classes of sources of widely varying X-ray to optical luminosities. We feel that this strategy rather than deep observations over small solid angles will determine  $\log N - \log S$  and the luminosity functions most accurately for the local epoch since for a given observing time and fixed instrumental parameters the number of observed sources greater than some statistical limit is maximized when the solid angle is maximized at a given completeness level for a photon limited experiment.

#### ACKNOWLEDGMENTS

We thank J. Swank for extensive discussions and her major contribution to the HEAO-1 analysis program. We thank J. Huchra, D. Schwartz, W.H.M. Ku and C. Forman-Jones for communicating results prior to publication and G. DeZotti and T. Maccacaro for interesting discussion and D. Schwartz for a careful reading of the manuscript.

T A B L E 1

(1)	(2)	(3)	(4)	(5)	(6)(7)	(8)	(9)	(10)	(11)	(12)
H008+105	2S007+107	1.64 .21	<1.35	1112W2	1 *	.0898 W3	2.175	12.9		
H0039-096	2A0039-096 4U0037-10	2.64 .24	3.21 .38	ABELL 85	6 *	.0499 HSM	2.500	7 .25	8.82	
H0054-015	2A0054-015 4U0050-01	1.74 .33	2.13 .35	ABELL 119	6 *	.0446 N	2.550	3.89	4.76	
H0111-149		1.49 .22	.93 .35		7		2.500			1
H0122-591	2A0120-591 4U0106-59	1.29 .18	1.38 .2	FAIRALL9	1 *	.0461 W3	2.175	2.63	2.81	
H0123-352	2A0120-353 4U0115-36	2.52 .19	1.04 .28	NGC526A	1 *	.018 W3	2.175	.772	.319	
H0206-019	H0206-019	1.34 .23	.87 .41	MKN590	1 *	.027 W1	2.175	0.91	0.59	
H0235-52	2A0235-52	2.12 .14	.99 .23		7					
H0256+134	2A0255+132 1M0254+132 4U0254+13	2.95 .24	3.03 .33	ABELL 401	6 *	.0748 H	2.480	18.3	18.8	
H0316-443	2A0316-443 4U0321-45	1.82 .19	1.07 .23	PKS0316-443	6 **	.09 MA	2.520	16.7	9.82	
H0335+096	2A0335+096 4U0344+11	1.14 .22	1.86 .35	0335+096	6 *	.04 SC	2.810	2.25	3.67	
H0342-538	2A0343-536 1M0328-524 4U0339-54	1.4 .16	1.42 .17	CA0342-538	6 *	.052 MQ	2.520	4.21	4.27	
H0411+104	2A0411+103 1M0405+100 4U0410+10	2.61 .3	2.66 .34	ABELL 478	6 *	.09 B	2.480	23.6	24.0	
H0430-616	2A0430-615 1M0426-635 4U0427-61	2.53 .11	2.88 .14	SERCIC04/6	6 *	.0601 V	2.480	10.1	11.4	
H0431-134	2A0431-136 4U0431-12	2.16 .29	1.73 .3	ABELL 496	6 *	.036 C2	2.520	3.09	2.48	
H0430+053	2S0430+05 4U0432+05	2.04 .25	1.53 .36	3C120	1 *	.033 DV	2.175	2.12	1.59	
H0548-322	1M0545-322 4U0543-31	1.7 .18	1.2 .25	PKS0548-322	3 *	.069 FD	2.675	9.64	6.80	
H0557-385	4U0557-38	1.36 .16	2.26 .21		1 *	.0334 MP	2.17500	1.62	2.70	

H0630-541	2A0626-541 4U0627-54	1.98 .18	2.23 .13	SC0630-541	6 *	.0502 V	2.520	5.55	6.25	2
H0906-095	2A0906-095 4U0900-09	3.96 .28	4.16 .26	ABELL 754	6 *	.0537 C1	2.440	12.3	12.9	
H0917-074		1.36 .28	1.21 .3		7		2.500			
H0943-141	2A0943-140 4U0937-12	3.14 .25	3.97 .54	NGC2992	2 *	.0062 DV	2.175	.114	.143	
H0952+699	2A0954+700 1M0943+712 4U0954+70	1.32 .2	1.17 .2	M82	2 *	.0013 DV	2.480	.0024	.0021	
H1019+203	A1021+198	1.71 .24	.96 .3	NGC3227	2 *	.0033 W1	2.175	.0175	.0098	
H1034-273	2A1033-270 4U1033-26	2.19 .21	2.25 .3	ABELL 1060	6 *	.0114 M	2.880	.355	.365	
H1136-375	2A1135-373 4U1136-37	1.95 .23	<.6	NGC3783	1 *	.0091 W1	2.175	.152		
H1208+397	2A1207+397 1M1207+397 4U1206+39	6.34 .26	10.64 .36	NGC4151	1 *	.0033 W1	2.070	.0607	.104	
H1219+305	2A1219+305	1.61 .25	1.3 .3	1219+305	3 *		2.340		89.6	
H1226+023	2A1225+022 4U1226+02	3.46 .26	3.8 .37	3C273	5 *	.158 MS	2.040	81.6		
H1228+127	2A1228+125 1M1228+127 4U1228+12	14.2 .33	14.25 .33	VIRGO CL.	6 *	.0037 DV	2.850	.239	.240	
H1238-049	4U1240-05	1.71 .26	1.09 .41	NGC4593	1 *	.0085 DV	2.175	.116	.0741	
H1246-410	2A1246-410 1M1247-410 4U1246-41	5.15 .23	5.64 .37	CEN CL.	6 *	.0118 FO	2.740	.851	.932	
H1256-171		1.45 .28	<1.8	ABELL 1644	6 *	.0449 HSM	2.520	3.24		
H1257-042		1.47 .27	1.41 .53	ABELL 1651	6 **	.0826 HSM	2.520	11.3	10.9	
H1257+283	2A1257+283 1M1257+281 4U1257+28	14.67 .28	16.1 .32	ABELL 1656	6 *	.023 N	2.440	8.25	9.05	
H1324-311	2A1326-311 1M1329-314 4U1325-31	2.83 .25	2.74 .45	SC1326-31	6 *	.073 L	2.520	17.0	16.4	3
H1325-020		1.47 .25	<1.0		7		2.500			
H1332-336	2S1333-34	2.12 .18	2.59 .35	MC66-30-15	1 *	.006 W3	2.175	.0717	.0876	
H1344-333 7	2A1344-325	3.23 .27	2.49 .37	SC1344-32	6 **	.0144 L	2.520	.732	.565	

H1347+268	2A1346+266 4U1348+25	2.36	.25	2.91	.4	ABELL 1795	6 *	.0621	H	2.520	10.2	12.6
H1346-300	2A1347-300	3.7	.21	3.43	.37	IC4329A	1 *	.0138	W1	2.175	.665	.616
H1411-031	2A1410-029 1M1410-030 4U1410-03	2.69	.22	2.62	.43	NGC5506	2 *	.0056	DV	2.175	.0793	.0772
H1416+256	2A1415+255 4U1415+25	2.92	.23	2.77	.32	NGC5548	1 *	.0166	W1	2.175	.760	.721
H1508+060	2A1508+062 1M1514+068	3.00	.29	2.35	.36	ABELL 2029	6 *	.0767	F	2.520	19.9	15.6
H1513+070 CONFUSED? WITH 2A1519+082	1.51	.28	1.9	.36	ABELL 2052	6 *	.0344	M	2.520	1.97	2.48	
H1521+282	2A1518+274 4U1521+28	1.25	.2	1.69	.33	ABELL 2065	6 *	.0721	S	2.520	7.30	9.87
H1556+274	2A1556+274 4U1556+27	3.14	.24	2.87	.23	ABELL 2142	6 *	.0903	H	2.420	27.9	25.5
H1600+161	2A1600+164 4U1601+15	1.82	.23	2.	.41	ABELL 2147	6 *	.0377	N	2.740	3.11	3.42
H1627+396	2A1626+396 4U1627+39	2.72	.18	2.82	.24	ABELL 2199	6 *	.0312	N	2.740	3.17	3.29
H1630+057	2A1630+057 4U1636+05	1.26	.24	<1.8			7			2.500		
H1652+398	4U1651+39	1.01	.18	1.71	.28	MKN501	3 *	.034	DV	2.340	2.14	2.03
H1707+788	2A1705+786 1M1706+785 4U1707+78	2.53	.12	2.42	.1	ABELL 2256	6 *	.0603	F	2.480	10.1	9.68
H1829-591	4U1830-60	1.55	.21	.71	.24		7			2.500		
H1834-653		1.36	.18	1.08	.23	ESO103-G35	1 **	.013	W3	2.175	.217	.172
H1846-786	1M1849-781 4U1916-79	1.33	.16	1.48	.21		7			2.500		
H1917-587	2A1914-589 4U1924-59	1.70	.17	1.64	.26	ESO141-G55	1 *	.0368	W2	2.175	2.20	2.12
H2009-569	2A2009-569	3.19	.21	3.09	.25	SC2008-569	6 *	.06	B2	2.520	12.8	12.4
H2041-109	2A2040-115	2.08	.24	2.41	.31	MKN509	1 *	.0355	W1	2.175	2.50	2.73
H2154-304	2A2151-316	4.30	.24	2.33	.32	PKS2155-304	3 *	.17	CTB	2.525	146.	79.1



H2151-605	2A2155-609	1.29	.21	1.35	.25	STR2159-602	6	**	.1008	WF	2.520	14.9	15.6
	1M2140-602												
	4U2126-60												
H2158-321	2A2151-316	2.00	.23	1.4	.29	NGC7172	4	**	.009	DV	2.570	.180	.126
H2209-471		1.07	.21	1.83	.28	NGC7213	1	*	.0058	DV	2.175	.0338	.0578
H2216-027	2A2220-022	1.55	.24	.98	.29	3C445	2	**	.0562	OKP	2.175	4.71	2.98
H2233-261	2A2237-256	1.39	.22	1.94	.3	NGC7314	2	**	.0056	DV	2.175	.0410	.0572
H2301+086	2A2259+085	1.77	.25	1.45	.39	NGC7469	1	*	.0167	W1	2.175	.466	.382
	4U2300+08												
H2302-090	2A2302-088	1.88	.25	2.3	.34	MC62-58-22	1	*	.0479	W2	2.175	4.14	5.06
	4U2305-07												
H2316-426	2A2315-428	2.51	.23	3.04	.29	NGC7582	2	*	.0048	DV	2.175	.0543	.0658
H2342+089	4U2344+08	1.31	.27	.93	.33	ABELL2657	6	*	.0414	N	2.520	2.49	1.77

COLUMN CAPTIONS:

- (1) : H NAME
- (2) : PREVIOUS NAMES
- (3) : 1ST SCAN FLUX AND 1-SIGMA ERROR (R15 COUNTS/SEC)
- (4) : 2ND SCAN FLUX AND 1-SIGMA ERROR (R15 COUNTS/SEC)
- (5) : IDENTIFICATION
- (6) : TYPE OF OBJECT: 1 = SEYFERT 1 GALAXY  
2 = SEYFERT 2, NELG, N OR OTHER ACTIVE GALAXY  
3 = BL LACERTE OBJECT  
4 = NORMAL GALAXY  
5 = QSO  
6 = CLUSTER OF GALAXIES  
7 = UNIDENTIFIED
- (7) : QUALITY OF IDENTIFICATION: \* = CERTAIN; SAS-3 OR HEAD-1 MODULATION COLLIMATOR POSITION OR EINSTEIN OBSERVATORY POSITION  
\*\* = POSSIBLE
- (8) : REDSHIFT VALUE AND REFERENCE:  
B = BAHCALL, N.A., SARGENT, W.L.W., 1977, AP.J., 217, L19  
B2 = BAHCALL, N.A., AP.J., 217, L77  
C1 = CORWIN, H.G.JR., 1971, PUBL.ASTRON.SOC.PACIFIC, 83, 320  
C2 = CORWIN, H.G.JR., 1974, A.J., 79, 1356  
CMR = CANIZARES, C.R., MCCLINTOCK, J.E., RICKER, G.R., 1978, AP.J., 226, L1  
CTB = CHARLES, P., THORSTENSEN, J., BOWYER, S., 1979, NATURE, 281, 285  
DV = DEVAUCOULEURS, DEVAUCOULEURS AND CORWIN SECOND REFERENCE CATALOG OF BRIGHT GALAXIES 1976  
F = FABER, S., DRESSLER, A., 1977, A.J., 82, 167  
FD = FOSBURY, R.A.E., DISNEY, M.J., 1976, AP.J., 207, L75  
FO = FORMAN, W., JONES, C., TANANBAUM, H., 1976, AP.J., 206, L29  
H = HINTZEN, P., SCOTT, J.S., 1979, AP.J., 232, L145

HSM = HINTZEN, P. SCOTT, J. S., MCKEE, J. D., 1980 AP. J. IN PRESS  
 L = LUGGER, P., 1978, AP. J., 221, 745  
 M = MELNICK, J., SARGENT, W., 1977, AP. J., 215, 401  
 MA = MACCAGNI, D., TARENGHI, M., COOKE, B. A., MACCACCARO, T., PVE, J. P., RICKETTS, M. J., CHINCARINI, G., 1978, ASTRON. & ASTROPHYS., 62, 127  
 MP = MELNICK, J., QUINTANA, H., 1975, AP. J., 198, L97  
 MQ = MCHARDY, J. AND PVE, J. IAU CIRCULAR 3587 1981  
 MS = SCHMIDT, M., 1968, AP. J., 151, 393  
 N = NOONAN, T., 1973, A. J., 78, 26  
 OKP = OSTERBROK, D. E., KOSKI, A. T., PHILLIPS, M. M., 1976, AP. J., 206, 898  
 S = SPINRAD, H., 1977, PUB. A. S. P., 89, 116  
 SC = SCHWARTZ, D., SCHWARZ, J., TUCKER, W., 1980, AP. JLETT. 238, L59  
 V = VIDAL, N. V., 1975, PUBL. ASTRON. SOC. PACIFIC, 87, 625  
 W1 = WEEDMAN, D. W., 1977, ANN. REV. ASTRON. ASTROPHYS., 15, 69  
 W2 = WEEDMAN, D. W., 1978, MON. NOT. R. ASTR. SOC., 184, 11P  
 W3 = WEEDMAN, D. W., 1979, PROC. IAU GENERAL ASSEMBLY, MONTREAL  
 WF = WEST, R. M., FRANSEN, S., 1980, ESO SCIENT. PREPRINT N. 110,

(9) : CONVERSION FACTOR (1.E-11 ERGS/CM2 SEC PER R15 COUNTS/SEC)

(10) : 1ST SCAN LUMINOSITY (1.E44 ERGS/SEC)

(11) : 2ND SCAN LUMINOSITY (1.E44 ERGS/SEC)

(12) : NOTES

1. IPC DETECTION BUT NOT IDENTIFIED AT PRESENT
2. MULTIPLE CLUSTER FORMAN ET AL 1981
3. MULTIPLE CLUSTERS PERRENOD AND HENRY 1981



## REFERENCES

- Avni, Y., Bahcall, J.N. 1980, Ap. J. 235, 694.
- Bahcall, N. 1979, Ap. J. 232, 639.
- Birnbaum, Z.W., Tingey, F.M. 1951, Ann. Math. Stat 22, 592.
- Boldt, E. 1980, Invited Talk at AAS Meeting, NASA TM 80659.
- Bradt, H., Doxsey, R.E., and Jernigan, J.G. 1979, Advances in Space  
Exploration.
- Charles, P. Thorstensen, J., Bowyer, S., and Middleditch, J. 1979, Ap. J.  
(Letters) 231, L131.
- Crawford, D.E., Jauncy, D.L., Murdoch, H.S. 1970, Ap. J. 162, 405.
- DeVaucouleurs, G. 1958, A.J. 63, 253.
- DeVaucouleurs, G., DeVaucouleurs, A. and Corwin, H. 1976, Second Reference  
Catalog of Bright Galaxies, Univ. of Texas Press.
- DeZotti, G. 1980, preprint.
- Doxsey, R., McClintock, J., Petro, L., Remillard, R., and Schwartz, D. 1981  
B.A.A.S. 13, 558.
- Elvis, M., Maccacaro, T., Wilson, A., Ward, M., Penston, M., Fosbury, R.,  
Perola, G. 1978, MNRAS 183, 129.
- Fabian, A.C. and Rees, M.J. 1978, MNRAS 185, 109.
- Forman, W., Bechtold, J., Blair, W., Giacconi, R., Van Speybroeck, L, and  
Jones, C. 1981, Ap. J. (Letters) 243, L133.
- Garcia, M., Baliunas, S.L., Conroy, M., Johnston, M.D., Ralph, E., Roberts,  
W., Schwartz, D.A., and Tonry, J. 1980, Ap. J. (Letters) 240, L107.
- Garcia, M., Conroy, M., Doxsey, R., Griffiths, R.E., Johnston, M., Ralph, E.,  
Roberts, W., and Schwartz, D.A. 1980, BAAS 12, 527.
- Giacconi, R., Bechtold, J., Branduaradi, G., Forman, W., Henry, J.P., Jones,  
C., Kellogg, E., van der Laan, H., Liller, W., Marshall, H., Murray,

S.S., Pye, J., Schreier, E., Sargent, W.G.W., Seward, F., and Tananbaum,  
H. 1979, Ap. J. (Letters) 234, L1.

Griffiths, R.E., Ward, M.J., Blades, J.C., Wilson, A.S. 1979, Ap. J. 232, L27.

Griffiths, R.E., Lamb, D.Q., Ward, M.J., Wilson, A.J., Charles, P.A.,  
Thorstensen, J., McHardy, I.M. and Lawrence, A. 1980, MNRAS 193, 25p.

Holt, S.S. 1980, invited talk at Cambridge HEAD meeting, NASA TM 82010.

Huchra, J.P. and Sargent, W.L.W. 1973, Ap. J. 186, 433.

Huchra, J.P. 1977, Ap. J. Suppl. 35, 171.

Huchra, J.P. 1980, private communication.

Kriss, G.A., Canizares, C.R., and Ricker, G.R. 1980, Ap. J. 242, 492.

Lightman, A., Hertz, P., and Grindlay, J.E. 1980, Ap. J. 241, 367.

Marshall, F.E., Boldt, E.A., Holt, S.S., Mushotzky, R.F., Pravdo, S.H.,  
Rothschild, R.E., and Serlemitsos, P.J. 1979, Ap. J. (Suppl) 40, 657.

Marshall, F.E., Boldt, E.A., Holt, S.S., Miller, R., Mushotzky, R.F., Rose,  
L.A., Rothschild, R., and Serlemitsos, P.J. 1980, Ap. J. 235, 4.

McHardy, I. 1978, MNRAS 182, 760.

McKee, J., Mushotzky, R., Boldt, E., Holt, S., Marshall, F.E., Pravdo, S., and  
Serlemitsos, P. 1980, Ap. J. 242, 843.

Murdoch, H.S., Crawford, D.F., and Jauncey, D.L. 1973, Ap. J. 183, 1.

Mushotzky, R.F. 1979, Proceedings of the Erice Symposium on X-Ray Astronomy,  
eds. R. Giacconi and G. Setti, p. 171.

Mushotzky, R., Marshall, F.E., Boldt, E., Holt, S., and Serlemitsos, P. 1980,  
Ap. J. 235, 36.

Perrenod, S. and Henry, J.P. 1981, preprint.

Pye, J.P. and Warwick, R.S. 1979, MNRAS 187, 905.

Rothschild, R., Boldt, E., Holt, S., Serlemitsos, P., Garmire, G., Agrawal,  
P., Riegler, G., Bowyer, S., and Lampton, M. 1979, Space Science

- Instrumentation 4, 265.
- Schwartz, D.A. 1978, Ap. J. 222, 8.
- Schwartz, D.A., Bradt, H., Briel, V., Doxsey, R.E., Fabbiano, G., Griffiths, R.E., Johnston, M.D., Margon, B. 1979, Ap. J. 84, 1560.
- Schwartz, D.A., 1979 in (COSPAR) X-Ray Astronomy, W.A. Baity and L.E. Peterson (eds), Pergamon Press, Oxford and New York, p.453.
- Schwartz, D.A. 1980, private communication.
- Swank, J., Boldt, E.A., Holt, S.S., Rothschild, R.E., and Serlemitsos, P.J. 1978, Ap. J. (Letters) 226, L133.
- Swank, J., Lampton, M., Boldt, E., Holt, S., and Serlemitsos, P. 1977, Ap. J. (Letters) 216, L71.
- Tananbaum, H., Peters, G., Forman, W., Giacconi, R., Jones, C., and Avni, Y. 1978, Ap. J. 223, 74.
- Tsikoudi, V. and Swank, J. 1981, in preparation.
- Van Speybroeck, L., Epstein, A., Forman, W., Giacconi, R., Jones, C., Liller, W., and Smarr, L. 1979, Ap. J. 234, L45.
- Warwick, R.S. and Pye, J.P. 1978, MNRAS 183, 169.
- Weedman, D. 1979, Invited Talk at Montreal IAU General Assembly.
- Weinberg, S. 1972, Gravitation and Cosmology
- West, R.M., and Frandsen, S. 1980, ESO Scientific Preprint, No. 110.
- White, N.E., Sanford, P.W., and Weiler, E.J. 1978, Nature 274, 569.
- Worrall, D., Boldt, E., Holt, S., Mushotzky, R., and Serlemitsos, P. 1981, Ap. J. 243, 53.

## FIGURE CAPTIONS

Figure 1. The completeness level of the present survey vs ecliptic latitude. The diamonds are for the first pass and the crosses for the second pass. The lower histogram is the sky fraction in each ecliptic latitude bin (right hand scale). The centre of the diamonds and crosses is 5 times the mean error for a source located in that ecliptic latitude bin and the size of the error bar is the standard deviation of this error. Since we truncate at 1.25 R15 counts all of our sources at ecliptic latitude greater than  $30^\circ$  lie well above the 5 $\sigma$  level. We estimate that residual incompleteness of sources at levels less than 1.4 cts is less than 3 sources and zero sources greater than this limit.

Figure 2. The error boxes for H0328+025 and H0917-074. The inner and outer boxes are the 90% confidence boxes as described in Marshall et al. 1979. The inner box assumes that the source was roughly constant during our period of observation.

Figure 3. The distribution of the non-galactic sources detected in this survey in supergalactic coordinates.

Figure 4. The probability distributions for  $\kappa$  and  $\alpha$ . The top panel shows the AML probability vs.  $\alpha$  in the first pass data, the middle panel shows the AML probability vs.  $\alpha$  in the second pass. The bottom panel shows the 68 and 95% joint probability contour for  $\kappa$  and  $\alpha$  for the first pass data. The + marks the best fit.

Figure 5. The differential  $\log N - \log S$  distribution for our sample. The best fit is indicated. The highest flux point is indicated by a dashed cross because its upper flux bound is not well defined. (1st pass data)

Figure 6. The AML Kolomogorov-Smirnov test distribution for an  $\alpha = 2.5$  model. The 50 and 95% probability bounds are indicated. (1st pass data)

Figure 7. The ratio of the number of observed sources  $N_{\text{Obs}}$  to the number of expected sources for  $\alpha = 2.5 \log N - \log S$  law. (1st pass data)

Figure 8a. The cluster of galaxies differential luminosity function for the first pass data.

8b. The same information for the second pass data. The best fit power law models are indicated on both panels.

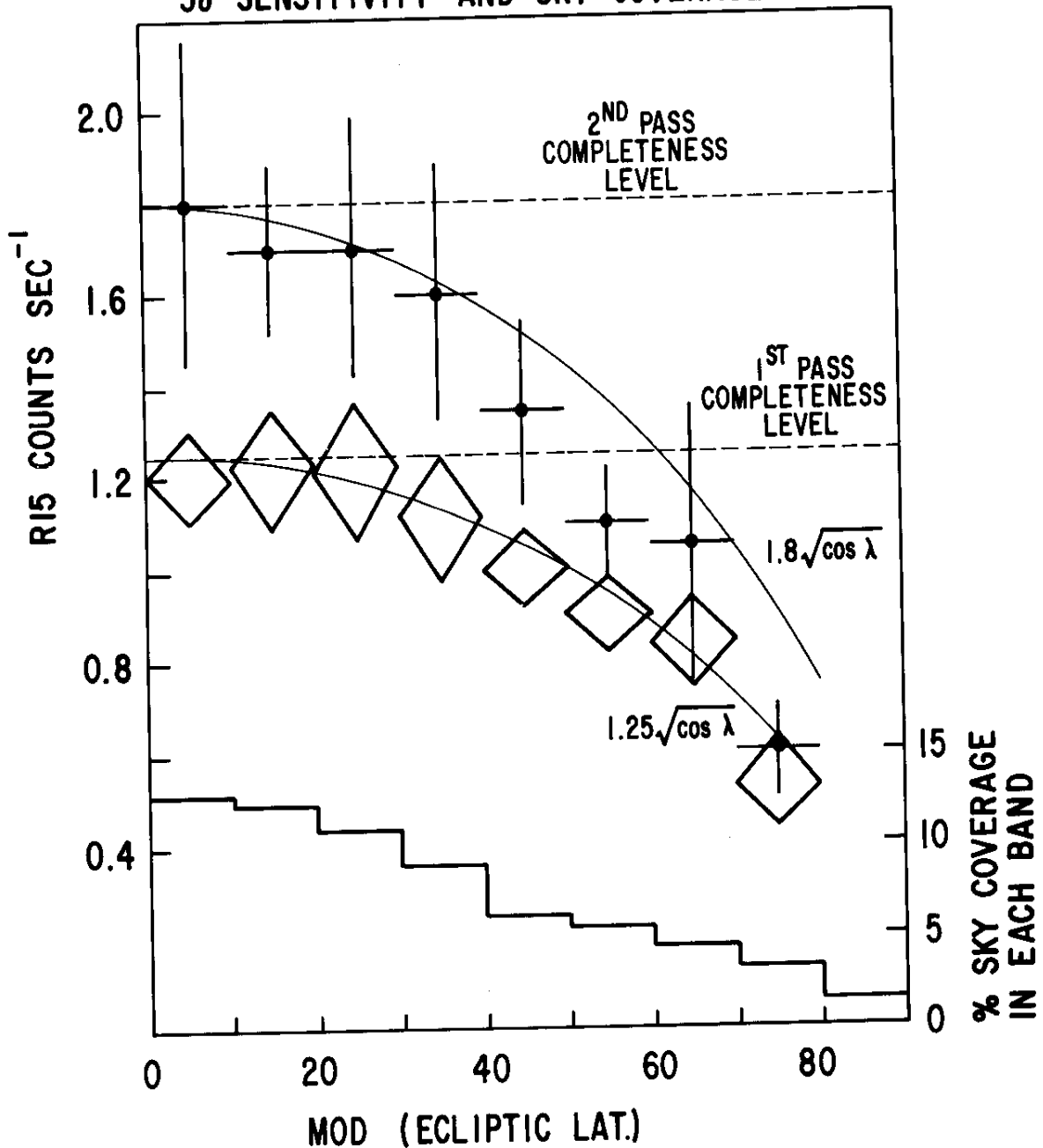
Figure 9. the AML probability vs.  $\gamma$  the slope of the power law differential luminosity function for clusters of galaxies for the first and second passes including and excluding the Virgo cluster.

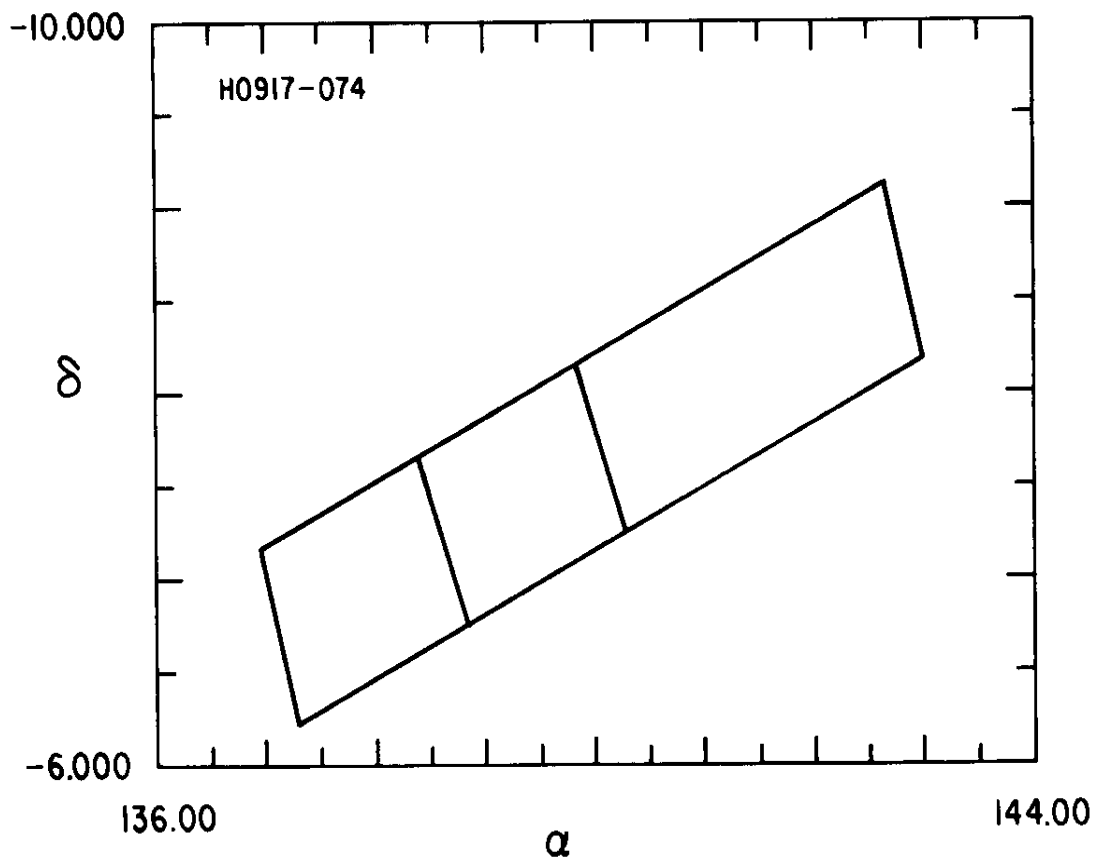
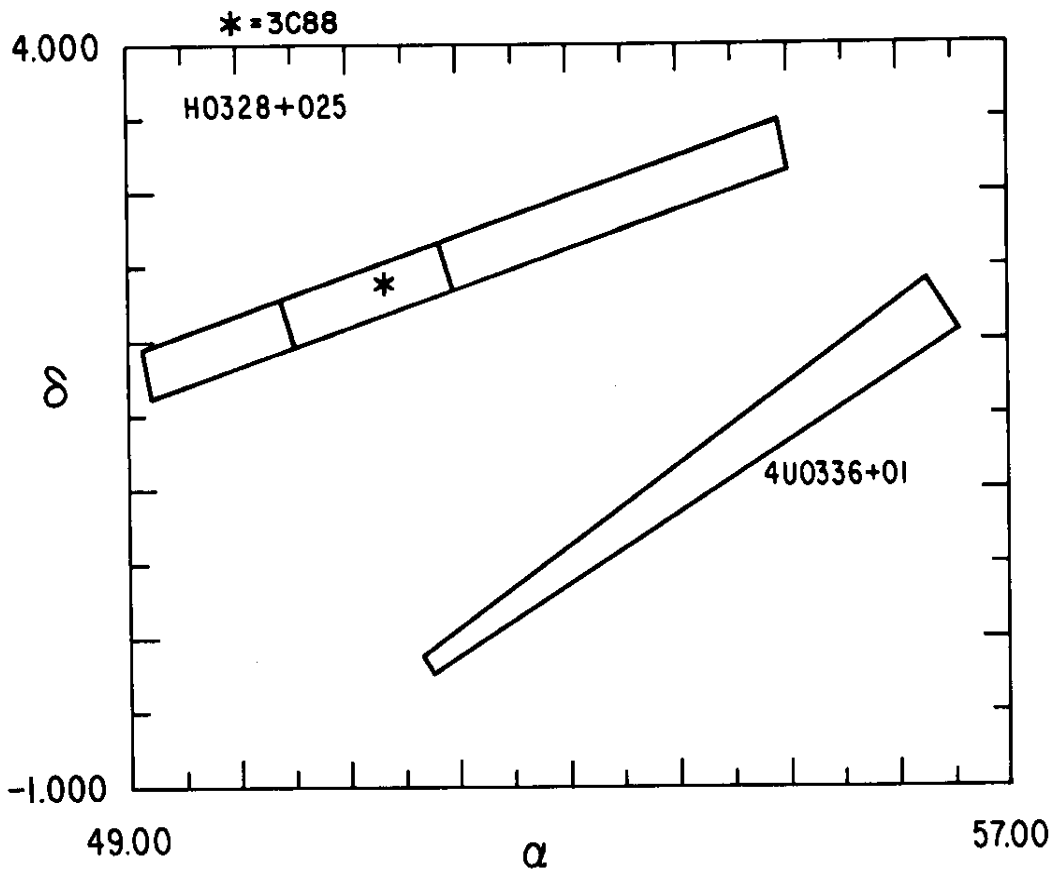
Figure 10. Same as Figure 9 but for the exponential luminosity function..

Figure 11. The Seyfert galaxy luminosity function for the first pass data. The best fit power law differential model is indicated. The insert shows the AML probability vs.  $\gamma$  the slope of the luminosity function.

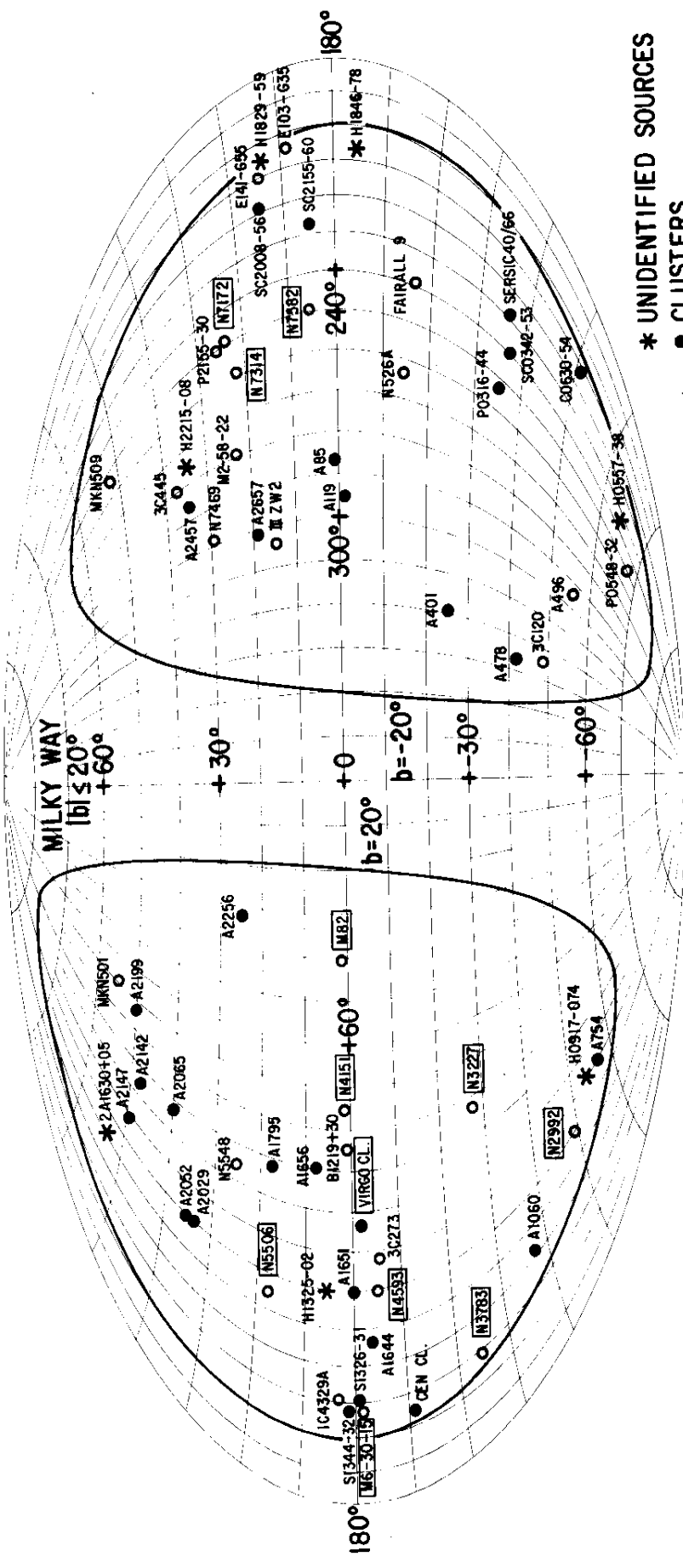


# 5 $\sigma$ SENSITIVITY AND SKY COVERAGE



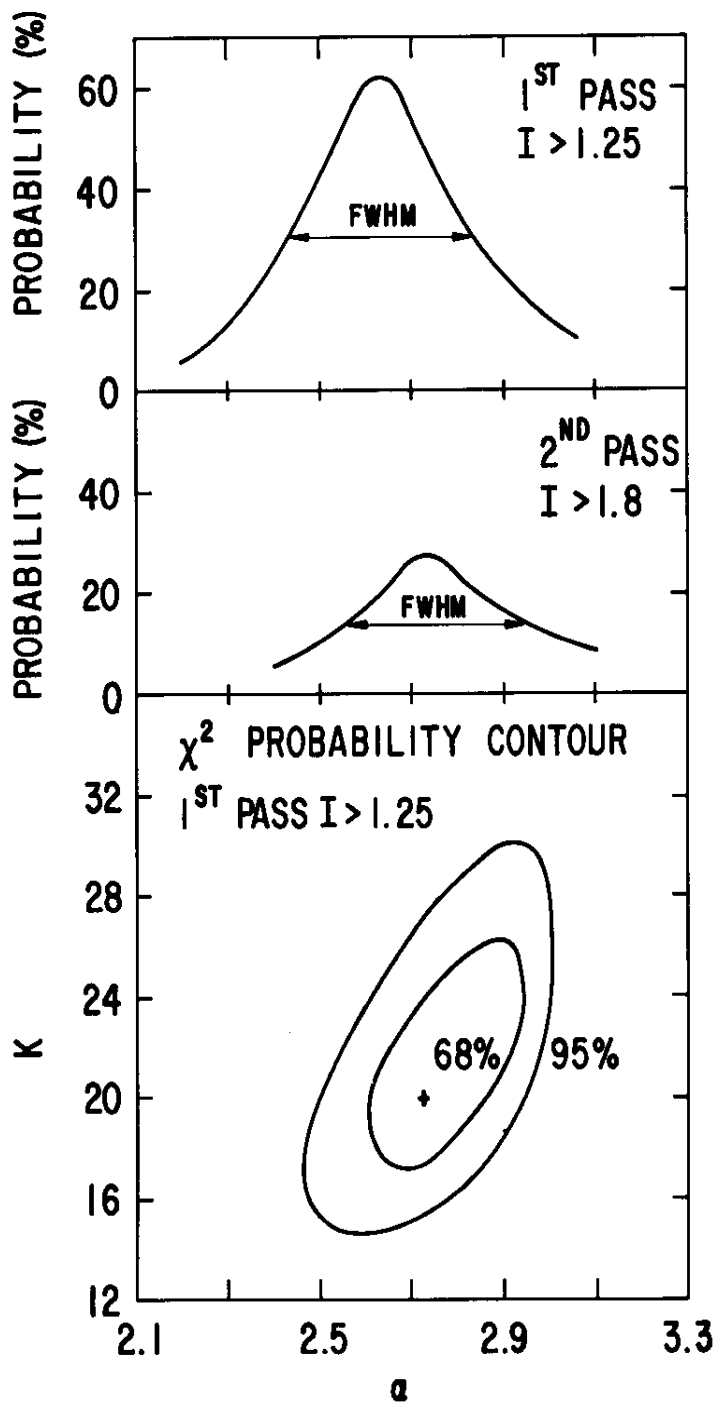


SUPERGALACTIC COORDINATES

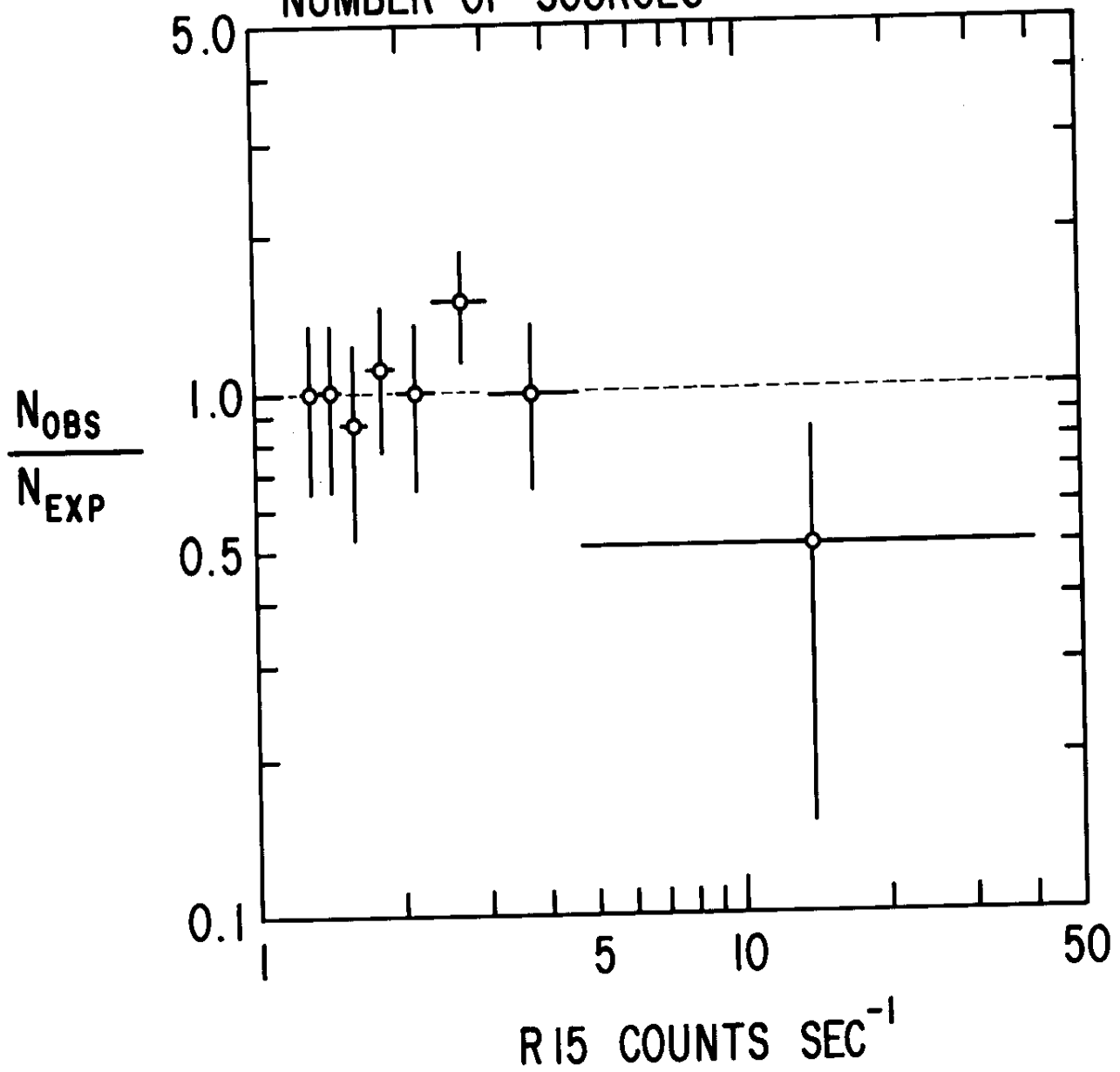


- \* UNIDENTIFIED SOURCES
- CLUSTERS
- GALAXIES
- Z ≤ 0.01

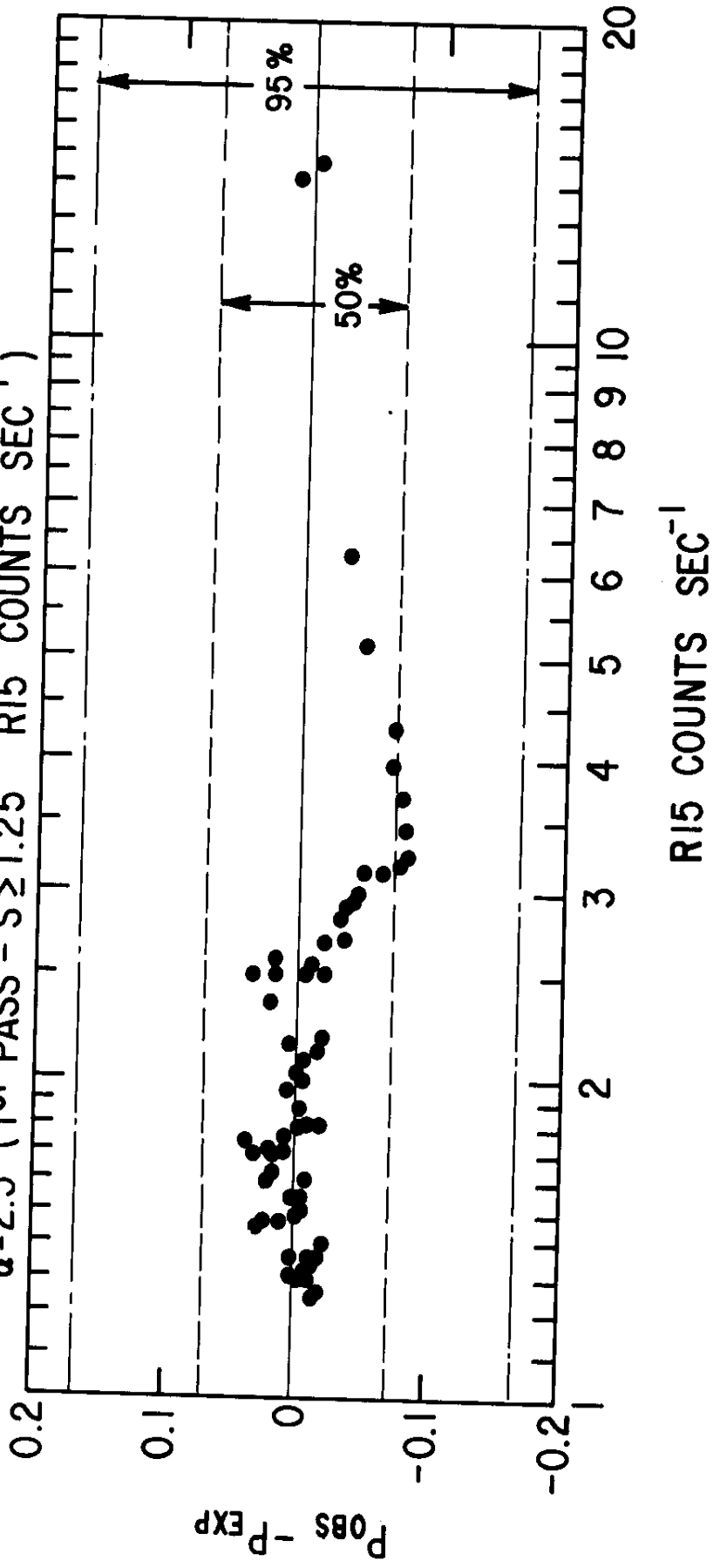
S > 1.25 RI5 COUNTS SEC<sup>-1</sup>



RATIO OF OBSERVED TO EXPECTED  
NUMBER OF SOURCES

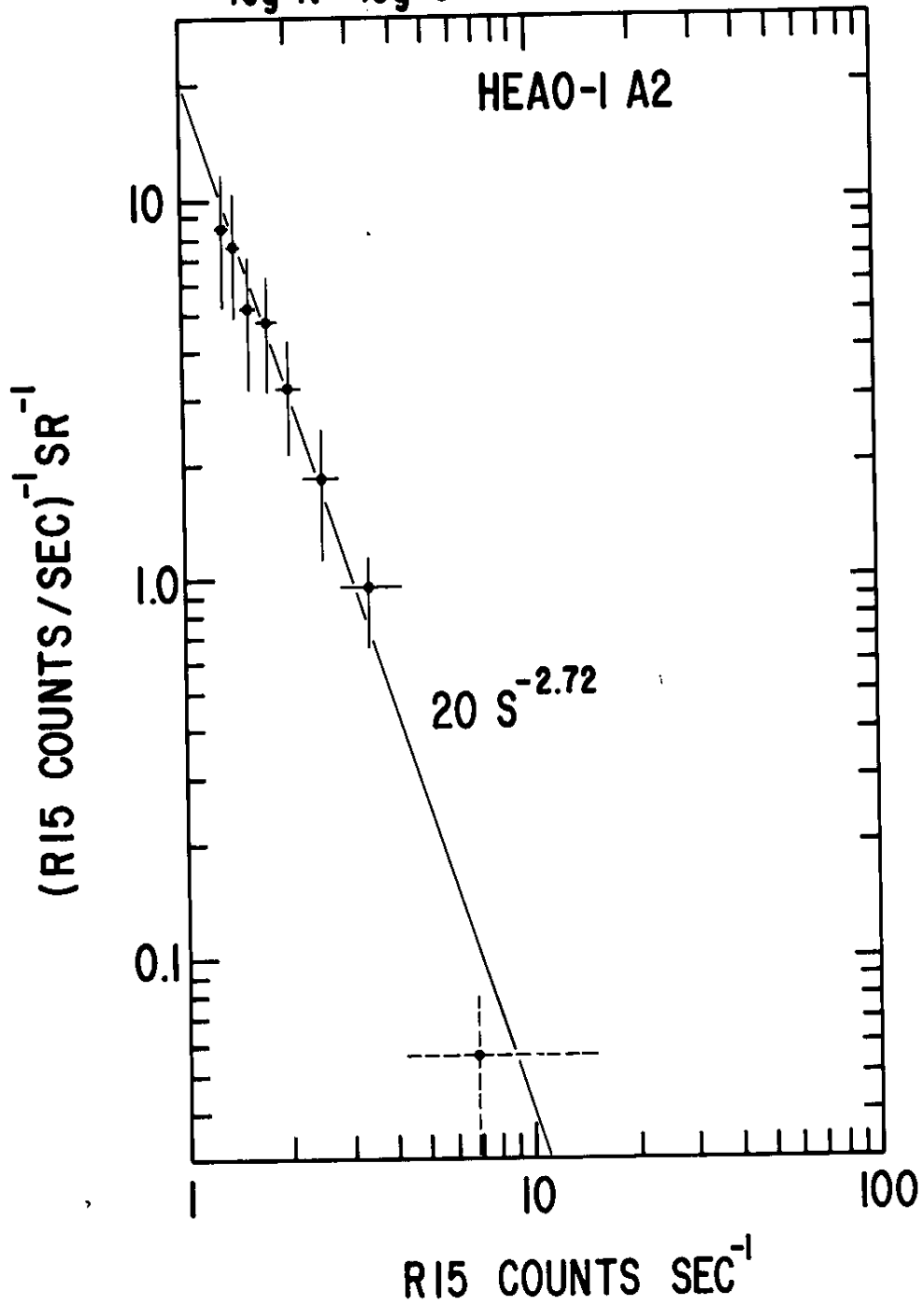


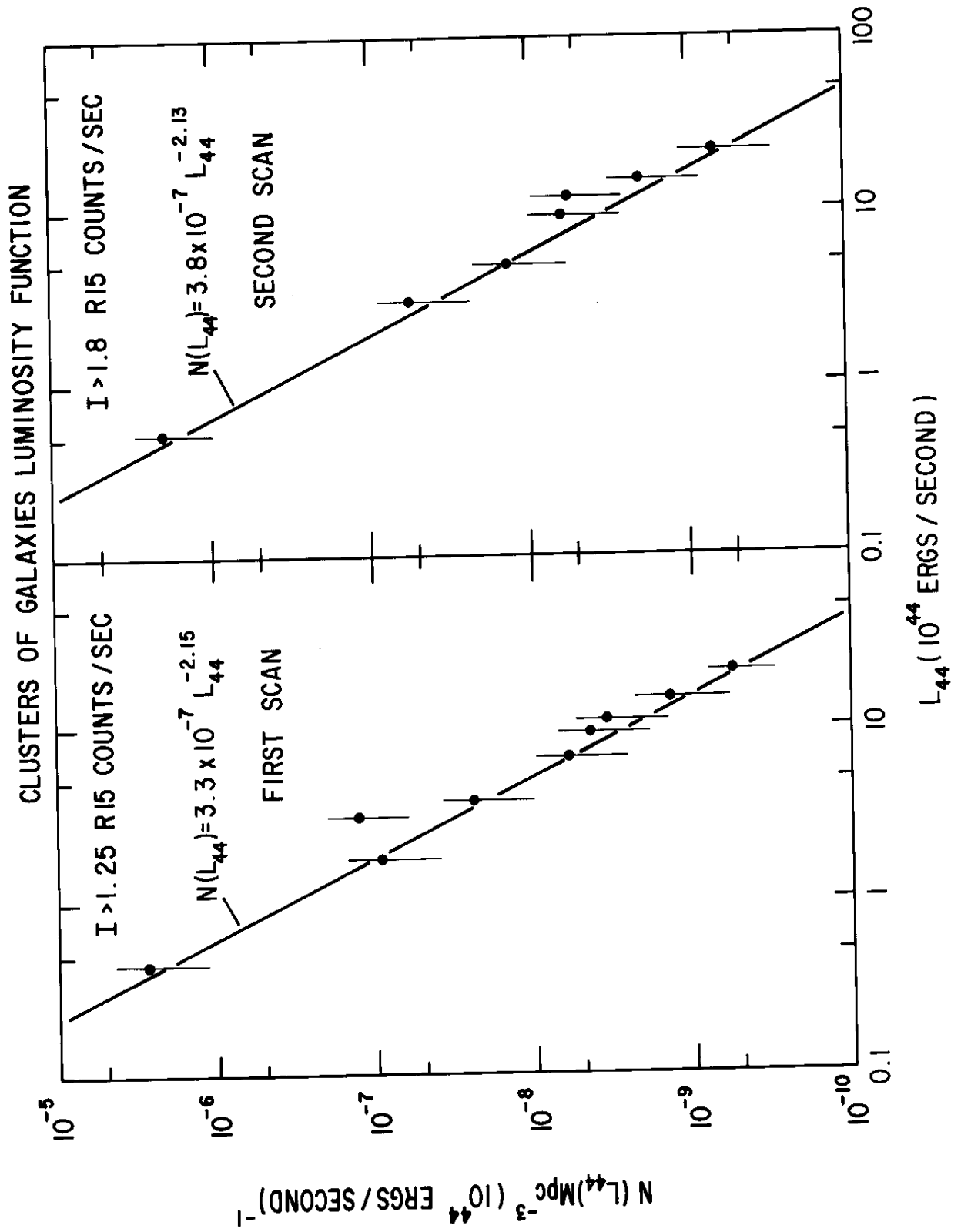
AML - KS TEST FOR EUCLIDEAN MODEL:  
 $\alpha = 2.5$  (1ST PASS -  $S \geq 1.25$  RI5 COUNTS SEC<sup>-1</sup>)



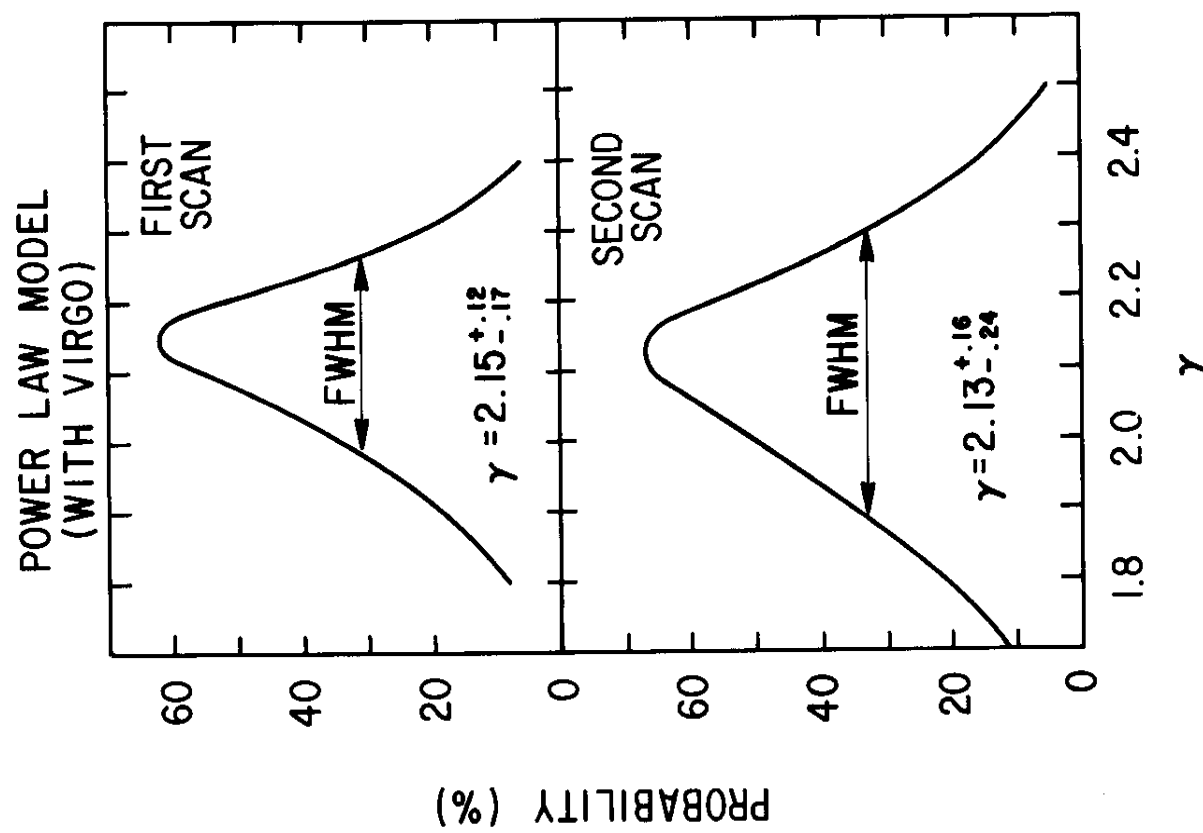
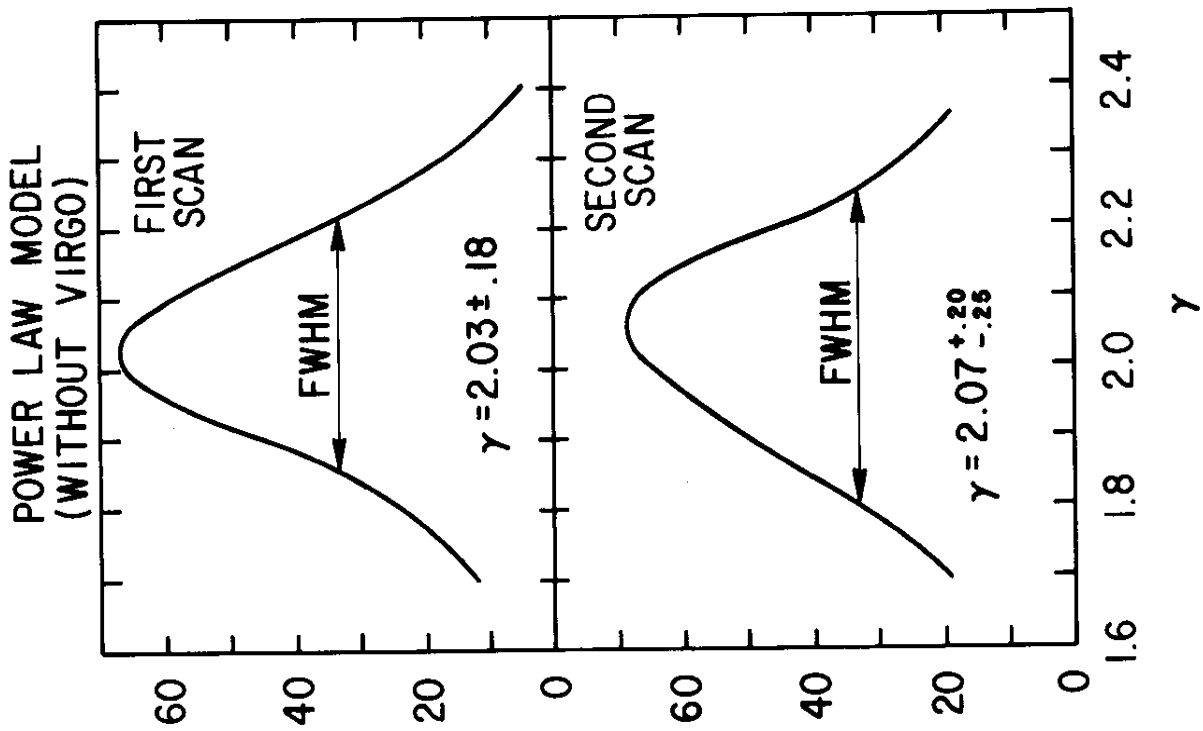
# log N - log S DISTRIBUTION

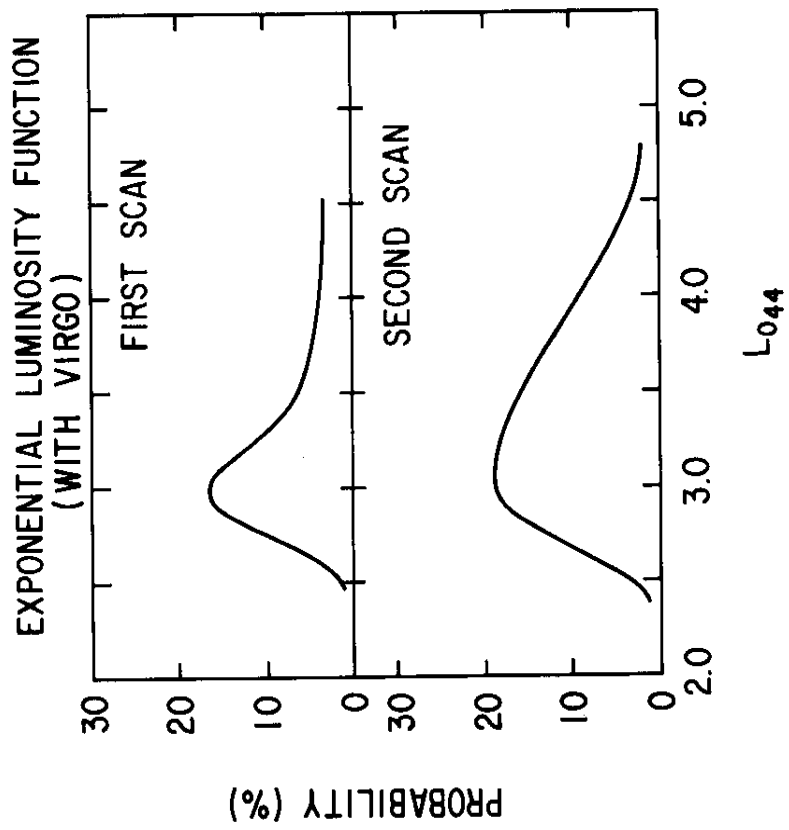
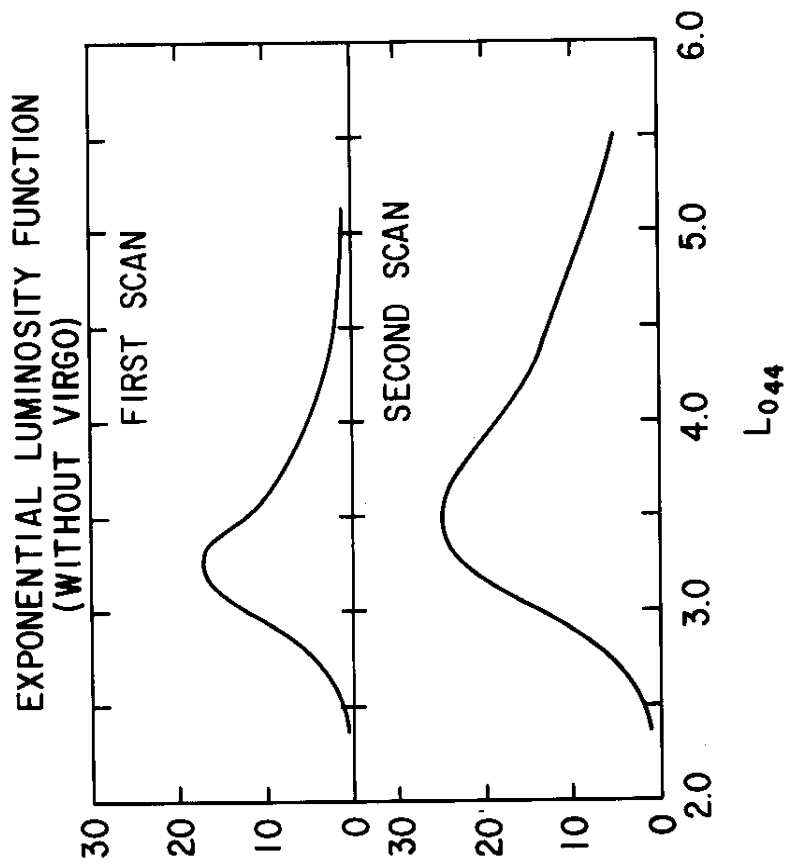
HEAO-1 A2



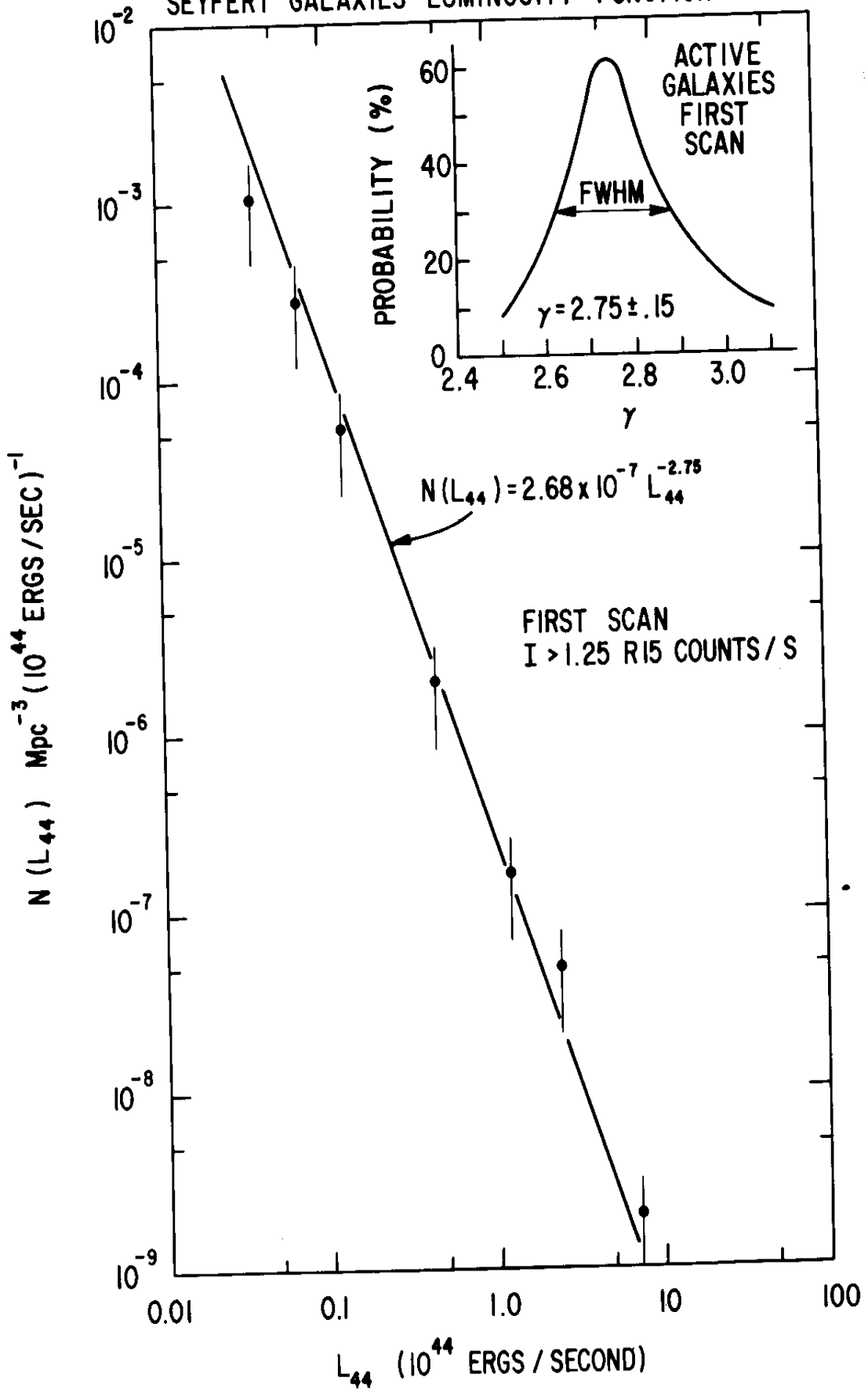








# SEYFERT GALAXIES LUMINOSITY FUNCTION



## BIBLIOGRAPHIC DATA SHEET

1. Report No. TM 82168	2. Government Accession No.	3. Recipient's Catalog No.	
4. Title and Subtitle A Complete X-Ray Sample of the High Latitude ( $ b  > 20^\circ$ ) Sky from HEAO-1 A-2: Log N - Log S and Luminosity Functions		5. Report Date August 1981	
		6. Performing Organization Code 661	
7. Author(s) G. Piccinotti, R. Mushotzky, E. Boldt, S. Holt, F. Marshall, P. Serlemitsos, R. Shafer		8. Performing Organization Report No.	
9. Performing Organization Name and Address Code 661 Cosmic Radiations Branch Laboratory for High Energy Astrophysics NASA/Goddard Space Flight Center Greenbelt, Maryland 20771		10. Work Unit No.	
		11. Contract or Grant No.	
		13. Type of Report and Period Covered	
		14. Sponsoring Agency Code	
12. Sponsoring Agency Name and Address			
15. Supplementary Notes  Accepted for publication in The Astrophysical Journal			
16. Abstract  The HEAO-1 experiment A-2 has performed a complete X-ray survey of the 8.2 steradians of the sky at $ b  > 20^\circ$ down to a limiting sensitivity of $< 3.1 \times 10^{-11}$ ergs/cm <sup>2</sup> sec in the 2-10 keV band. Of the 85 detected sources (excluding the LMC and SMC sources) 17 have been identified with galactic objects, 61 have been identified with extragalactic objects and 7 remain unidentified. The log N - log S relation for the non-galactic objects is well fit by the Euclidean relationship. We have used the X-ray spectra of these objects to construct log N - log S in physical units. The complete sample of identified sources has been used to construct X-ray luminosity functions, using the absolute maximum likelihood method, for clusters of galaxies and active galactic nuclei.			
17. Key Words (Selected by Author(s)) X-Ray Sources, Luminosity Function, Cosmic X-Ray Background		18. Distribution Statement	
19. Security Classif. (of this report) U	20. Security Classif. (of this page) U	21. No. of Pages 48	22. Price*

INPUT PARAMETERS ARE: AS FL=5=5 1

TAPE NO. 1 FILE NO. 1  
RECORD 1 TABLE 1 LENGTH 2400

(2) (3) (4) (5) (6) (7) (8) (9) (10) (11)

1112W2 1 \* .0898 W3 2.175 12.9 H0008+105 2S0007+107 1.64 .21 <1.35  
 96 2A0039-096 2.54 .24 3.21 .38 ABELL 85 6 \* .0499 HSM 2.500 7 .25 H0039-0  
 8.82 4U0037-10

2.13 .35 ABELL 119 6 \* .0446 N 2.550 3.89 H0054-015 2A0054-015 1.74 .33  
 4U0050-01

500 H0111-149 1 1.49 .22 .93 .35 7 2.  
 1.38 .2 FAIRALLS 1 \* .0461 W3 2.175 2.63 H0122-591 2A0120-591 1.29 .1  
 4U0106-59

TAPE NO. 1 FILE NO. 1  
RECORD 2 2A0120-353 LENGTH 2400  
 H0123-352 .319 2.52 .19 1.04 .28 NGC5264 1 \* .018 W3 2.175  
 .772

.23 .87 .41 MKM590 1 \* .027 W1 2.175 0.91 H0206-019 H0206-019 1.34  
 H0235-52 2A0235-52 2.12 .14 .99 .23 7

.33 ABELL 401 6 \* .0748 H 2.480 18.3 H0256+134 2A0255+132 2.95 .24 3.03  
 1M0254+132 4U0254+

13  
 443 6 \* .09 MA 2.520 16.7 H0316-443 2A0316-443 1.82 .19 1.07 .23 PKS0316-  
 4U0321-45

0335+096 2A0335+096 1.14 .22 1.86 .35 0335+096 6 \* .04 SC 2.810 2.2  
 3.67 4U0344+11 H0342-538 2A0343-536 1.4 .1  
 4U0339-54

6 1.42 .17 CA0342-538 6 \* .052 MQ 2.520 4.21 H0342-538 2A0343-536 1.4 .1  
 1M0328-524

TAPE NO. 1 FILE NO. 1  
RECORD 3 LENGTH 2400  
 H0411+104 2A0411+103 2.61 .3 2.66 .34 ABELL 478 6 \* .

0-46893  
 9/15/77 - 9/11/78  
 Turn open is not  
 to in the denominator.

----- H0430-616 2A0430-615 2.53 .11 2.88 .14 SERVIC40/6 6 \* .0601 V 2.480  
10.1 11.4 1M0426-635 4U0427-61

34 2A0431-136 2.16 .29 1.73 .3 ABELL 496 6 \* .036 C2 2.520 H0431-1  
2.48 4U0431-12

----- 1.53 .36 3C120 1 \* .033 DV 2.175 2.12 H0430+053 2S0430+05 2.04 .25  
4U0432+05

----- FD 2.675 H0548-322 1M0545-322 1.7 .18 1.2 .25 PKS0548-322 3 \* .069  
9.64 4U0543-31

----- 0557-38 1.36 .16 2.26 .21 1 \* .0334 MP 2.17500 1.62 H0557-385 4U  
2.70

TAPE NO. 1 FILE NO. 1  
RECORD 4 LENGTH 2400  
H0630-541 6.25 2A0626-541 1.98 .18 2.23 .13 SC0630-541 6 \* .0502 V 2.520  
5.55 4U0627-54

----- .28 4.16 .26 ABELL 754 6 \* .0537 C1 2.440 12.3 H0906-095 2A0906-095 3.96  
4U0900-09

----- 2.500 H0917-074 1.36 .28 1.21 .3 H0943-141 2A0943-140  
7

3.14 .25 3.97 .54 NGC2992 2 \* .0062 DV 2.175 .114 H0943-141 2A0943-140  
4U0937-

----- 2 \* .0013 DV 2.480 .0024 .0021 1M0943+712 1.32 .2 1.17 .2 M82  
4U0954+70

----- 3 W1 2.175 H1019+203 A1021+158 1.71 .24 .96 .3 NGC3227 2 \* .003  
.0175 .0098

----- 1 2.25 .3 ABELL 1060 6 \* .0114 M 2.880 .355 H1034-273 2A1033-270 2.19 .2  
4U1033-26

TAPE NO. 1 FILE NO. 1  
RECORD 5 LENGTH 2400  
H1136-375 2A1135-373 1.95 .23 <.6 NGC3783 1 \* .0091 W1 2.175  
.152 4U1136-37

----- .26 10.64 .36 NGC4151 1 \* .0033 W1 2.070 .0607 .104 2A1207+397 6.34  
1M1207+397  
4U1206+39

----- .3 1219+305 3 \* 2.340 H1219+305 2A1219+305 1.61 .25 1.3  
H1226+0

----- 23 2A1225+032 3.46 .26 3.8 .37 3C273 5 \* .158 MS 2.040 81.6  
H1226+0

89.6 4U1226+02

14.25 .33 VIRGO CL. 6 \* .0037 DV 2.850 H1228+127 2A1228+125 14.2 14.2 .33

U1228+12

C4593 1 \* .0085 DV 2.175 .116 H1238-049 4U1240-05 1.71 .26 1.09 .41 NG  
1246-410 5.15 .23 5.64 .37 . CEN CL. 6 \* .0118 F0 2.740 H1246-410 2A  
1M1247-410 .851 .932

TAPE NO. 1 FILE NO. 1  
RECORD 10 LENGTH 2400

005 DV 2.570 .180 H2158-321 2A2151-316 2.00 .23 1.4 .29 NGC7172 4 \*\*  
1.83 .28 NGC7213 1 \* .0058 DV 2.175 .0338 H2209-471 1.07 .21  
H2216-027 2.98 2A2220-022 1.55 .24 .98 .29 3C445 2 \*\* .0562 OKP 2.175  
4.71  
.3 NGC7314 2 \*\* .0056 DV 2.175 .0410 H2233-261 2A2237-256 1.39 .22 1.94  
86 2A2259+085 1.77 .25 1.45 .39 NGC7469 1 \* .0167 W1 2.175 H2301+0  
.382 4U2300+08

2.3 .34 MCG2-58-22 1 \* .0479 W2 2.175 4.14 H2302-050 2A2302-088 1.88 .25  
8 DV 2.175 .0543 H2316-426 2A2315-428 2.51 .23 3.04 .29 NGC7582 2 \* .004  
7 .93 .33 ABELL2657 6 \* .0414 N 2.520 H2342+089 4U2344+08 1.31 .2

TAPE NO. 1 FILE NO. 1  
RECORD 11 LENGTH 2400

COLUMN CAPTIONS:

(1) : H NAME

(2) : PREVIOUS NAMES

(3) : 1ST SCAN FLUX AND 1-SIGMA ERROR (RIS COUNTS/SEC)

(4) : 2N

D SCAN FLUX AND 1-SIGMA ERROR (RIS COUNTS/SEC)

(5) : IDENTIFICATION

(6) : TYPE OF OBJECT: 1

= SEYFERT 1 GALAXY  
2 = SEYFERT 2, NELG, N OR OTHER ACTIVE GALAXY  
3 = BL LACERTE OBJECT  
4 = NORMAL GALAXY  
5 = QSO

6 = CLUSTER OF GALAXIES  
7 = UNIDENTIFIED

TAPE NO. 1 FILE NO. 1  
RECORD 12 LENGTH 2400

(7) : QUALITY OF IDENTIFICATION: \* = CERTAIN: SAS-3 OR HEAO-1 MODULATION COLL  
\*\* = POSSIBLE

VALUE AND REFERENCE: (8) : REDSHIFT

B = BAHCALL, N.A., SARGENT, W.L.W., 1977, AP.J., 217, L19  
B2 = BAHCALL, N.A., AP.J., 217, L77

CIFIC, 83, 320  
74, A.J., 79, 1356  
R = CANIZARE, S.C.R., MCCLINTOCK, J.E., RICKER, G.R., 1978, AP.J., 226, L11  
C1 = CORWIN, H.G., JR., 1971, PUBL. ASTRON. SOC. PA  
C2 = CORWIN, H.G., JR., 19  
CM

CTR = CHARLES, P., THORSTENSEN, J., BOWYER, S., 1979, NATURE, 281, 285  
DV = DEVAUCOULEURS, DEVAUCOULEURS AND CORWIN SECOND REFERENCE  
F = FABER, S., DRESSLER, A., 1977, A.J., 98  
FD = FOSBURY, R. A

E CATALOG OF BRIGHT GALAXIES 1976  
2, 167  
E, DISNEY, M.J., 1976, AP.J., 207, L75  
FO = FORMAN, W., JONES, C., TANANBAUM, H., 1976, AP.J., 206, L29  
H = HINTZEN, P., SCOTT, J.S., 1979, AP.J., 232, L145  
HSM = HINTZEN, P., SCOTT, J.S., MCKEE, J.D., 1980, AP.J., IN P  
L = LUGGER, P., 1978, AP.J., 221, 74  
M = MELNI

RESS  
5  
CK, J., SARGENT, W., 1977, AP.J., 215, 401  
MA = MACCAGNI, D., TARENGHI, M., COOKE, B.A., MACCAGARO, T., PYE, J.P., RICKETTS, M.J., CHINCARINI, G  
., 1978, ASTRON. ASTROPHYS

TAPE NO. 1 FILE NO. 1  
RECORD 13 LENGTH 2400  
MP = MCHARDY, J. AND PYE, J IAU CIRCULAR 3587 1981  
MS = SCHMIDT, M., 1968, AP.J., 151, 353  
N = NOONAN, T., 1973, A.J., 78,  
OKP = OS

26  
TERBRACK, D.E., KOSKI, A.T., PHILLIPS, M.W., 1976, AP.J., 206, 898  
S = SPINRAD, H., 1977, PUB. A.S.P., 89, 116  
SC = SCHWARTZ, D., SCHWARZ, J., TUCKER, W., 1980, AP.J., 238, L59  
V = VIDAL, N.V., 1975, PUBL. ASTRON. SOC. PACIFI  
M1 = WEEDMAN, D.W., 1977  
M2

C, 87, 625  
ANN, REV. ASTRON. ASTROPHYS., 15, 69  
= WEEDMAN, D.W., 1978, MON. NOT. R. ASTR. SOC., 184, 11P  
M3 = WEEDMAN, D.W., 1979, PROC. IAU GENERAL ASSEMBLY, MONTREAL  
MF = WEST, R.M., FRANSEN, S., 1980, ESO SCIEN. PREPRINT N.110

(1.E-11 ERGS/CM2 SEC PER R15 COUNTS/SEC) (9) : CONVERSION FACTOR

(10) : 1ST SCAN LUMINOSITY (1.E44 ERGS/SEC)

(11) : 2ND SCAN LUMINOSITY (1.E44 ERGS/SEC)

(12) : NOTES

TAPE NO. 1 FILE NO. 1  
RECORD 14 LENGTH 360

1. IPC DETECTION BUT NOT IDENTIFIED AT PRESENT  
2. MULTIPLE CLUSTER FORMAN ET AL 1981  
3. MULTIPLE CLUSTERS PERRENOD AND HENRY 1981